APPENDIX A

Express Mail Label No. EV957671572US Dated: July 20, 2007

Docket No.: UMY-055
(PATENT)

IN THE UNITED STATES PATENT AND TRADEMARK OFFICE

In re Patent Application of:
Michael P. Czech *et al.*

Application No.: 10/735461 Confirmation No.: 3119

Filed: December 11, 2003 Art Unit: 1635

For: METHOD OF INTRODUCING siRNA INTO ADIPOCYTES Examiner: R.A. Schnizer

MS Amendment
Commissioner for Patents
P.O. Box 1450
Alexandria, VA 22313-1450

DECLARATION PURSUANT TO 37 CFR §1.132

Dear Sir:

We, Michael P. Czech, Qiong L. Zhou, and Zhen Y. Jiang, are named inventors in the above-identified application and make this declaration in support thereof, and particularly in response to the February 22, 2007 Office Action. I, Michael P. Czech, am Professor and Chair of the Program in Molecular Medicine at the University of Massachusetts Medical School. I, Qiong L. Zhou, am an Instructor in the laboratory of Michael P. Czech at the University of Massachusetts Medical School. I, Zhen Y. Jiang, am a Research Assistant Professor in the laboratory of Michael P. Czech at the University of Massachusetts Medical School.

(1) We understand that the Examiner has maintained the rejection of claims 27, 44-48, 50, 51, 56-59, 79, and 81-83 under 35 U.S.C. § 103(a) as being unpatentable over Al-Hasani *et al.* (*J. Biol. Chem.* 273(28):17504-17510, 1998) in view of Clancy *et al.* (US20030087259); additionally in view of Paquereau *et al.* (*Anal. Biochem.* 204(1):147-151, 1992) for claims 38-43, 84, and 85; additionally in view of Standaert *et al.* (*J. Biol. Chem.* 272(48):30075-30082, 1997) for claim 49; and additionally in view of McSwiggen *et al.* (U.S. Patent No. 7,022,828) for claims 52-55.

(2) Al-Hasani *et al.* does not describe the transfection or electroporation of adipocytes with siRNA. Rather, Al-Hasani *et al.* describes the transfection of adipose cells with ***DNA and DNA expression plasmids*** in order to characterize the mechanism of GLUT4 endocytosis by overexpressing a dominant-negative mutant of dynamin-1 in rat adipose cells.

Clancy *et al.* teach diagnostic assays for detecting bone and cartilage formation and therapeutic methods for treating disease and disorders related to bone and cartilage formation or resorption. Clancy *et al.* teach siRNAs as potential agents for "blocking or reducing the expression of a gene or the activity or level of the encoded polypeptide that is modulated, *e.g.*, upregulated, during normal bone or cartilage formation" (see *e.g.*, para. 0239)).

There is no basis in Al-Hasani *et al.* in view of Clancy *et al.* for providing any reasonable expectation of success in electroporating adipocytes with siRNA, as claimed in the present invention, for the following reasons:

(a) One of ordinary skill in the art would not have been motivated to substitute the ***DNA plasmids*** transfected in Al-Hasani *et al.* with the ***siRNAs*** disclosed by Clancy *et al.* as an agent capable of blocking gene expression. The mere fact that Clancy *et al.* lists siRNAs and dominant negative mutants as potential gene blocking compounds in a more extensive list of gene blocking compounds, *e.g.*, antisense molecules, ribozymes, triplexes, aptamers, does not arise to the level of a motivation to select one specific member from the recited antagonist list for use in the featured methodology.

(b) One of ordinary skill in the art one would not have had a reasonable expectation that a substitution of the DNA plasmids of Al-Hasani *et al.* with the siRNAs disclosed by Clancy *et al.* would result in success. Specifically, it was well known in the art at the time of filing that electroporation of DNA into adipocytes only leads to the successful expression of DNA in only a small minority of the adipocytes (***approximately 1-10%***[1]). In contrast, in order for siRNA to successfully silence the gene of interest, *i.e.*, mediate RNA interference, as currently claimed, it is required that virtually all of the adipocytes (***approximately 100%***) take up functional siRNA. ***Since the successful electroporation of DNA into adipocytes is typically less than 10% efficient, it would <u>not</u> have been obvious to one of ordinary skill in the art at the time of filing of the instant invention that electroporation of siRNA into adipocytes would be nearly 100% efficient***[2].

[1] See, *e.g.*, page 40, lines 15-17 of the instant specification.

[2] Using labeled siRNA, Figure 1B, left panels, and Example 2, page 40, lines 1-17, of the specification demonstrate that the electroporation of siRNA into adipocytes was, unexpectedly, nearly 100% efficient.

A skilled artisan would have had an appreciation of these significant differences and would not have reasonably expected that mere substitution of the siRNAs of Clancy *et al.* for the plasmid DNAs transfected in Al-Hasani *et al.* would be successful.

(c) The secondary references of Paquereau *et al.*, Standaert *et al.*, and McSwiggen *et al.* fail to cure the deficiencies of the Al-Hasani and Clancy references. Specifically, Paquereau describes the transfection of ***hepatocyte cells with DNA***, Al-Hasani is describes the study of insulin stimulation in glucose transport by transfection of rat adipocytes ***with plasmid DNA***, and McSwiggen teaches the general use of modified siRNA oligonucleotides which modulate the expression or function of IKK genes, in several cell types, ***none of which include adipocytes***. Thus, these secondary references fail to rectify the deficiency of teachings of the Al-Hasani and Clancy references.

(3) The art is replete with teachings which support the non-obviousness of the present invention. Following are several examples demonstrating the difficulty of transfecting adipocytes with siRNA and the successful use of the present invention to electroporate adipocytes with siRNA:

(a) As demonstrated in Appendix A, in 2006 Robinson *et al.* state that "adipocytes are difficult to transfect, and until recently, successful siRNA transfection was achieved only via electroporation" (see, *e.g.*, page E885, second column, third full paragraph). Robinson *et al.* go on to cite a 2004 scientific publication of one of the inventors of the instant application, M. Czech, as the group which was successful in transfecting adipocytes with siRNA using electroporation.

(b) As demonstrated in Appendix B, the 2006 Panomics DeliverX Plus siRNA Transfection Kit Brochure discloses that "[t]ransfection of siRNA into differentiated 3T3-L1 adipocytes... has only been accomplished by electroporation" (see, *e.g.*, first page, left column) and specifically references the 2003 *Proceedings of the National Academy of Sciences* scientific publication by the instant inventors which corresponds to the instant patent application. This Brochure goes on to further disclose that "***adipocytes... represent one of the most difficult-to-transfect cell lines used routinely in cell biology studies***" (see, *e.g.*, page 2, right column, second full paragraph) (Emphasis added).

(c) As demonstrated in Appendix C, Jain discloses that "***adipocytes are fully differentiated cells with no proliferation and are thus difficult to transfect*** by either RNAi or ASO approaches" (see, *e.g.*, page 308, middle column, first paragraph) (Emphasis added).

(d) As demonstrated in Appendix D, Venugopal *et al.* disclose that "***adipocytes... proved difficult to transfect efficiently with siRNA***" (see, *e.g.*, page 17122, second column, first full paragraph) (Emphasis added).

(4) In conclusion, we hereby declare that there is no basis in Al-Hasani *et al.* in view of Clancy *et al.* for providing any reasonable expectation of success in electroporating adipocytes with siRNA, as claimed in the present invention. Furthermore, the secondary references of Paquereau *et al.*, Standaert *et al.*, and McSwiggen *et al.* fail to cure the deficiencies of the Al-Hasani and Clancy references.

We hereby declare that all statements made herein of our own knowledge are true and that all statements made on information and belief are believed to be true; and further that these statements were made with the knowledge that willful false statements and the like so made are punishable by fine or imprisonment, or both, under Section 1001 of Title 18 of the United States Code and that such willful false statements may jeopardize the validity of the application or any patent issued thereon.

Michael P. Czech, Ph.D. Date July 18, 2007

Qiong L. Zhou, Ph.D. Date July 18, 2007

Zhen Y. Jiang, Ph.D. Date July 18, 2007

APPENDIX B

RNAi and siRNA in target validation

Kewal K. Jain, Blaesiring 7, 4057 Basel, Switzerland, e-mail: jain@pharmabiotech.ch

Gene silencing by RNA interference (RNAi) technologies has made considerable progress in the last few years [1] and small interfering RNAs (siRNAs) have become a preferred modality for target validation, which was the theme of the *4th International Conference on RNAi and siRNA*, organized by IBC Life Sciences in Zurich, Switzerland from 3–4 February 2004.

Genomic and proteomic technologies have helped to discover a plethora of drug targets, in turn creating a bottleneck in the drug discovery process that is being tackled with target validation using RNAi technologies. However, the problems of delivery and off-target effects, as well as poor tissue distribution, present significant challenges, as pointed out by Clive Jackson of AstraZeneca (http://www.astrazeneca.com) in his opening talk. Success criterion at AstraZeneca is 85% of message knockout and this was achieved for a kinase in the synovial fibroblast. The Global Target Validation Network within AstraZeneca is monitoring the success of siRNA across the company in different biological systems and disease areas. The design of siRNA experiments draws on general observations on gene silencing studies with RNase H antisense as well as experience with siRNA sequence selection and delivery optimization. Jackson pointed out that it is often necessary to confirm function by alternative approaches to siRNA in a full target validation package.

Sumedha Jayasena of Amgen (http://www.amgen.com) reviewed the benefits and drawbacks of RNAi for target validation. Certain siRNAs can silence 'off-targets', induce an interferon response, silence chromatin and lead to false conclusions on end points. To maximize the benefits of using siRNA, Jayasena called for a better understanding of the mechanism of siRNA action, intelligent approaches to siRNA design and chemical modification, and better screening for non-specific effects. To avoid undesirable effects of siRNAs, one should identify highly potent siRNAs that can be effective at low nanomolar concentrations. Internal stability of siRNAs should be achieved during the design stage to reduce participation of the sense strand. Finally, chemical modification of siRNA can reduce or eliminate nonspecific and off-target effects.

RNAi in model systems

Andreas Köpke of Devgen (http://www.devgen.com) described the use of model systems for target validation and identification. *Caenorhabditis elegans* forms the basis of Devgen technology, which involves finding *C.elegans* homologs of potential human gene targets that require validation. Selective RNAi knockdown or knockout technology is applied to these genes to study expression patterns and a phenotypic profile is compiled. This information leads to the identification of pathways influenced by the target and its relevance for the disease. The advantages of this approach include the use of a genome-wide library for every assay, applicability throughout the life cycle, the controllable strength of knockdown, assay speed and low cost, although the disadvantages are that the degree of knockout can vary between genes and it is difficult to tackle neurological targets. Genes involved in obesity have been identified using this approach and mice with a targeted disruption of the stearoyl-CoA desaturase-1 (SCD-1) isoform have reduced body adiposity and increased insulin sensitivity [2]. A genome-wide RNAi screen identified druggable targets that reverse disease and two of these have progressed to lead selection. Validation of these targets has also been conducted in mammalian models using gene knockdown by lentiviral-mediated transduction of short hairpain RNA (shRNA). Christophe Echeverri of Cenix Bioscience (http://www.cenix.com) presented a multispecies platform using *C. elegans* and Drosophila, as well as human cells, for high-throughput RNAi; 94% of siRNAs passed a silencing potency test, which involved high-throughput–high content assays and targets such as kinases, G-protein-coupled receptors and phosphatases, whereas 6% were rejected, and class-focused libraries are available for kinases and G-protein coupled receptors.

An integrated approach

An integrated approach to gene silencing was presented by Bettina Möckel (QIAGEN; http://www.qiagen.com/siRNA). Four siRNA duplexes targeted against the gene of interest were designed using an advanced algorithm and stringent homology analysis. Möckel also discussed the RNAiFect transfection reagent, which is based on a lipid formula developed specially for transfection of siRNA into a wide range of eukaryotic cells. Using a state-of-the-art design algorithm licensed from Novartis Pharma, QIAGEN is increasing the success rate (% active siRNAs) of gene silencing to a high level. Based on this, QIAGEN will be providing two siRNAs against the gene of interest, with the guarantee that at least one of them will reduce gene expression of the target mRNA by at least 70%. This presentation indicated that approaches to gene silencing should take into

1359-6446/04/$ – see front matter PII: S1359-6446(04)03050-8

DDT Vol. 9, No. 7 April 2004

consideration design, synthesis and delivery of siRNA as well as downstream analysis, and the last two factors should be automated processes.

siRNA delivery issues

Hans Winkler of Johnson & Johnson (http://www.jnj.com) emphasized that the delivery into cells was still the biggest hurdle in using siRNA. Cationic liposomes are promising for this purpose but are toxic. Although polyamines and peptides are less toxic, they are difficult to attach to siRNA. MPG is derived from the fusion peptide domain of HIV-1 gp41 protein and MPG peptide–siRNA complexes have been used for *in vivo* acute silencing studies. Lentiviral vectors and herpes simplex viruses (HSV) are used as vectors for central nervous system targets. There is insufficient experience with transgenic expression of shRNA and it is limited mainly to Pol II promoters, which have no regulatory or tissue specificity. Winkler cited previous work showing that it is possible to express long double-strand RNA (dsRNA) from an RNA polymerase II (Pol II) promoter using a vector, named pDECAP [3] Because the transcripts from pDECAP lack both the 5′-cap structure and the 3′-poly(A) tail that facilitate dsRNA export to the cytoplasm, long dsRNA does not leave the nucleus and hence does not induce the interferon response. It was concluded that the *in vitro* potential of RNAi is being met but more phenotypic *in vivo* data is needed to make a final judgment on the utility of RNAi.

Antisense and RNAi

Tatjana Achenback (Aventis; http://www.aventis.com) discussed the *in vitro* applications of RNAi and antisense oligonucleotides (ASOs) as a means of target validation. Transfection protocols using FITC-labeled control siRNAs and ASOs show that even differentiated cells are susceptible to knockdown technologies. Mouse 3T3-L1 fibroblasts were used as an *in vitro* model of diabetes, which were changed into adipocytes by treatment with dexamethasone and insulin. However, adipocytes are fully differentiated cells with no proliferation and are thus difficult to transfect by either RNAi or ASO approaches. Moreover, RNAi in model systems for metabolism interferes with functional assays. A proposed solution for this situation is retroviral vectors for antisense delivery as an alternative to the use of lipid vectors. In most of the validation assays, siRNAs were found to be superior to ASOs owing to greater efficacy or lower toxicity but general problems of delivery, stability of proteins and cellular system were applicable to both approaches.

Adenoviral-mediated functional screening

The use of adenoviral vectors for the delivery of small RNAs into cells was discussed by Frank Weise of the Natural and Medical Science Institute, University of Tübingen (http://www.nmi.de). The endogenous adenoviral expression of short hairpin RNA (shRNA) acts as a precursor to the formation of siRNA. The infection protocol is standardized by multiple assays. Parallelization and miniaturization is achieved by immobilization of adenoviral vectors. Adenoviral-mediated knockout thus meets the requirement of functional genomics.

Functional screening of the genome can also be accomplished using arrayed adenoviral libraries, as discussed by Helmuth van Es of Galapagos Genomics (http://www.galapagosgenomics.com). SilenceSelect™ and FlexSelect™ platforms, which are being applied to core disease programs that include Alzheimer's disease, rheumatoid arthritis, osteoarthritis and osteoporosis.

Non-viral RNAi-mediated gene knockdown

James Hagstrom of Mirus Corporation (http://www.RNAinterference.com) described RNAi delivery to target tissues *in vivo* using intravascular delivery under hydrodynamic pressure. Following a single tail vein injection, endogenous gene knockdown of 15–40% was achieved in 30–70% of hepatocytes. The key issue with this approach is the identification of effective knockdown sequences of siRNA and shRNA. Non-viral particles (plasmid DNA) and synthetic vectors can be used for *in vivo* target validation using RNAi and for therapeutic delivery of RNAi, and siRNA-containing particles exhibited increased serum stability and decreased toxicity. As well as intravascular delivery, an injection can be made directly into tissues or, alternatively, aerosol instillation can be used. Mirus has developed a transfection reagent (TransIT-TKO), an amphipathic polyamine and lipid mixture, specifically designed for siRNA delivery *in vivo*. Formulations have also been designed and optimized for individual cell lines.

siRNA-based therapeutics

Although RNAi is a dominant target validation technology, little effort has yet been made in the development of siRNA-based therapeutics. Nassim Usman of Sirna Therapeutics (http://www.sirna.com) reviewed preclinical studies of chemically modified siRNAs in animal models. Sirna is developing RNAi-based therapeutics that selectively target disease-causing genes and viruses. The focus is on developing siRNAs that target vascular endothelial growth factor for the treatment of macular degeneration.

Another company that is developing therapeutic applications for RNAi is Intradigm Corporation (http://www.intradigm.com). Patrick Lu described Intradigm's approach for siRNA delivery to disease models, particularly tumors via systemic delivery. siRNA can be used for the validation of tumorigenic targets as well as for therapeutic development and because siRNA is highly

sequence-specific, selective knockdown of tumor-causing mutants has tremendous therapeutic potential.

Concluding remarks

This was an excellent conference that included important contributions from several experts over two days. The advantages and limitations of RNAi approaches to the important topic of target validation were discussed. More importantly, measures were suggested to remedy some of the drawbacks of the new technologies.

References

1 Jain, K.K. (2004) *RNAi: technologies, markets and companies.* Jain PharmaBiotech Publications, Basel

2 Ntambi, J.M. et al. (2002) Loss of stearoyl-CoA desaturase-1 function protects mice against adiposity. *Proc. Natl. Acad. Sci. U. S. A.* 99, 11482–11486

3 Shinagawa, T. and Ishii, S. (2003) Generation of Ski-knockdown mice by expressing a long double-strand RNA from an RNA polymerase II promoter. *Genes Dev.*17, 1340–1345

4 Lu, P.Y. et al. (2003) siRNA-mediated antitumorigenesis for drug target validation and therapeutics. *Curr. Opin. Mol. Ther.* 5, 225–234

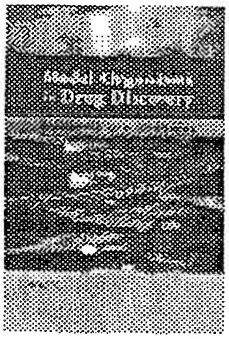

Model organisms in drug discovery

Edited by Pamela M. Carroll and Kevin Fitzgerald, Wiley Europe, 2003, 302 pages in hardback, ISBN: 0-470-84893-6

Over the past decade, huge advances in science have been made in areas such as genomics and proteomics, including, most significantly, the completion of the draft human genome sequence. Additionally, there has been an increase in spending in the pharmaceutical industry. However, these monumental steps forward have to date had little impact on our ability to combat and cure many human diseases and over the last ten years the number of marketable drugs has not significantly increased.

The process of getting a drug to market is long and arduous. Many promising targets and drugs fail along the way, costing time and millions of dollars. The process involves identifying and then validating a target, ultimately in human clinical trials, which still take the same amount of time as they did in years past. However, many inroads have been made in trying to shorten the time taken to identify targets and the use of model organisms has helped in this regard. These systems provide several advantages, including available genetic and molecular tools, cost, and short reproductive and generation times. Additionally, experiments in model systems are conducted in an intact organism.

Model systems have been used for decades for scientific study. Often, they provide an advantage for processes that seem too complex for study in more complex eukaryotes. Additionally, many of these studies have been groundbreaking (for example, the discovery of cell death genes in *Caenorhabditis elegans*), opening up new areas of study in mammals, including humans. Recently, many drug companies have begun to use model organisms as a faster, cheaper method to identify new drug targets. In the new book edited by Carroll and Fitzgerald, the use of model organisms in drug discovery is reviewed.

The book begins with a brief overview and comparison of each model system discussed in the book. The chapters are then organized in such a way as to start from the simplest to the most complex organism when compared with humans, including budding yeast (*Saccharomyces cerevisiae*), nematodes (*C. elegans*), flies (*Drosophila melanogaster*), zebrafish (*Danio rerio*) and mice (*Mus musculus*). Chapters are written by a researcher from the pharmaceutical field who has worked or works with that organism and provides details on almost all of the methods that have been or can be used for that organism in the pursuit of drug discovery. Moreover, both the advantages and disadvantages of the organism in this effort are discussed. Chapter 3 is particularly enlightening because the authors discuss in great detail how one goes from model system to target identification and validation using *C. elegans* as a model for unipolar depression.

This book is an invaluable resource for any researcher in the academic or private sector looking to expand into a model organism work because it reviews all available techniques for each model system. This is both an advantage as well as a limitation because, at times, chapters provide too little detail and are more like a good survey of available experimental techniques. However, this book should also be essential for any graduate level course on drug discovery or any researcher wanting to understand how model systems can be used in the laboratory.

The availability and understanding of model organisms might provide new tools for both academic researchers and drug companies. One watches the next few years with interest to see if this impacts on our ability to combat the complex diseases that ail our society.

Heidi A. Tissenbaum
Program in Gene Function and Expression
Program in Molecular Medicine
University of Massachusetts Medical School
Aaron Lazare Research Building Suite 615
364 Plantation Street
Worcester, MA 01605, USA
email: heidi.tissenbaum@umassmed.edu

1359-6446/04/$ – see front matter PII: S1359-6446(04)03049-1

APPENDIX C

Identification and modulation of a caveolae-dependent signal pathway that regulates plasminogen activator inhibitor-1 in insulin-resistant adipocytes

Joshi Venugopal*, Kazuhiko Hanashiro*†, Zhong-Zhou Yang, and Yoshikuni Nagamine‡

Friedrich Miescher Institute for Biomedical Research, Novartis Research Foundation, Maulbeerstrasse 66, 4058 Basel, Switzerland

Edited by Anthony Cerami, The Kenneth S. Warren Institute, Kitchawan, NY, and approved October 15, 2004 (received for review July 21, 2004)

Plasminogen activator inhibitor-1 (PAI-1) plays an important role in the pathogenesis of obesity-driven type 2 diabetes mellitus and associated cardiovascular complications. Here, we show that perturbation of caveolar microdomains leads to insulin resistance and concomitant up-regulation of PAI-1 in 3T3L1 adipocytes. We present several lines of evidence showing that the phosphatidylinositol 3-kinase (PI3K) pathway negatively regulates PAI-1 gene expression. Insulin-induced PAI-1 gene expression is up-regulated by a specific inhibitor of PI3K. In addition, serum PAI-1 level is elevated in protein kinase Bα-deficient mice, whereas it is reduced in p70 ribosomal S6 kinase 1-deficient mice. The PI3K pathway phosphorylates retinoblastoma protein (pRB), known to release free E2 (adenoviral protein) factor (E2F), which we have previously demonstrated to be a transcriptional repressor of PAI-1 gene expression. Accordingly, cell-penetrating peptides that disrupt pRB–E2F interaction, and thereby release free E2F, are able to suppress PAI-1 levels that are elevated during insulin-resistant conditions. This study identifies a caveolar-dependent signal pathway that up-regulates PAI-1 in insulin-resistant adipocytes and proposes a previously undescribed pharmacological paradigm of disrupting pRB–E2F interaction to suppress PAI-1 levels.

diabetes

Type 2 diabetes mellitus (T2DM) is characterized by insulin resistance, where the insulin receptor (IR) fails to elicit the metabolic signaling that is required for glucose metabolism and energy homeostasis. In insulin-sensitive tissues, the IR transduces two main signaling cascades: a metabolic signaling that is responsible for glucose uptake and glycogen synthesis and a mitogenic signaling that is responsible for cell proliferation and growth. The IR substrate (IRS)–phosphatidylinositol 3-kinase (PI3K)–protein kinase B (PKB) and Cbl-CAP-Flotillin pathways represents the major metabolic signaling, whereas the Shc-Ras-extracellular regulated kinase (Erk) pathway represents the major mitogenic signaling (1). Both in animal models and clinical T2DM subjects, a selective impairment of metabolic signaling has been observed, whereas mitogenic signaling is more or less unaffected (2–4).

Obesity is prominent among the plethora of factors that leads to the development of T2DM, although the molecular mechanism underlying the pathogenesis of obesity-driven T2DM is not well understood. Comparative analysis of large and small fat cells within the same fat pad reveals a 2-fold reduction in the levels of plasma membrane cholesterol in large fat cells, suggesting that a decrease in membrane cholesterol is characteristic of adipocyte hypertrophy per se (5). Recently, it has been proposed that the protein levels of caveolin-1 and -3 are inversely correlated to the body-mass index.[§] Plasma membrane cholesterol (6) and caveolins (7) are indispensable for the structural and functional integrity of caveolar microdomains. We therefore reasoned that obesity might lead to caveolar dysfunction. Because the IR and several of its downstream signal transducers are localized in caveolae (8), it was intriguing to investigate whether caveolar dysfunction could lead to insulin resistance.

There is compelling evidence that plasminogen activator inhibitor-1 (PAI-1), whose levels are elevated in both obesity and T2DM, plays an important role in the development of cardiovascular disorders (9). PAI-1, a primary physiological inhibitor of plasminogen activators (uPA and tPA), inhibits both fibrinolysis and proteolysis and plays an important role in mediating the cardiovascular complications associated with T2DM such as nephropathy (10), retinopathy (11), coronary artery disorders (12), and hypertension (13). Consequently, it is believed that normalizing plasma PAI-1 levels will retard the progression of cardiovascular complications (14). Insulin-induced Erk phosphorylation, followed by the activation of transcription factors of the AP-1 family, is considered to be partly, if not wholly, responsible for insulin-induced PAI-1 up-regulation in insulin-sensitive tissues (15, 16). However, because the mitogenic mitogen-activated protein kinase pathway is not affected during hyperinsulinemic conditions, such as insulin resistance or T2DM, this pathway is unlikely to be the primary cause of PAI-1 elevation during these pathological conditions. It is, therefore, intriguing to investigate whether insulin induction of PAI-1 during T2DM can be explained by directly linking the compromised PI3K pathway to PAI-1 up-regulation. Interestingly, it has been shown that IR-mediated activation of metabolic signaling (PI3K pathway) induces the phosphorylation of retinoblastoma protein (pRB) in adipocytes (17). pRB phosphorylation is known to lead to the release of free E2 (adenoviral protein) factor (E2F) (18). We have demonstrated (19) that E2F transcription factors can negatively regulate PAI-1 gene expression by repressing PAI-1 promoter activity independently of its binding to pocket proteins, revealing a novel mechanism for the E2F-mediated repression of gene expression. In this study, we investigate whether caveolar dysfunction can lead to insulin resistance, and whether the resulting impairment of the PI3K-PKB-E2F pathway can by itself lead to the up-regulation of PAI-1. We also explore the pharmacological disruption of the E2F–pRB interaction to release free E2F, which we hypothesize will attenuate PAI-1 transcription and hence its plasma level. Adipocytes are chosen for this study, because they are responsible for obesity, abundant in caveolae (20), highly sensitive to insulin (>200,000 receptors per cell) (21), the primary site for

This paper was submitted directly (Track II) to the PNAS office.

Abbreviations: PAI-1, plasminogen activator inhibitor-1; PI3K, phosphatidylinositol 3-kinase; PKB, protein kinase B; S6K1, p70 ribosomal S6 kinase 1; pRB, retinoblastoma protein; E2F, E2 (adenoviral protein) factor; MBCD, methyl-β-cyclodextrin; IR, insulin receptor; IRS, IR substrate; Erk, extracellular regulated kinase; T2DM, type 2 diabetes mellitus; siRNA, small interfering RNA; NIH-IR, NIH 3T3 cells overexpressing the human IR.

*J.V. and K.H. contributed equally to this work.

†Present address: First Department of Physiology, School of Medicine, University of the Ryukyus, Okinawa 903-0215, Japan.

‡To whom correspondence should be addressed. E-mail: nagamine@fmi.ch.

§Maianu, L., Chen, Y., Simmons, A., Wallace, P., Hutto, A., Shaughnessy, S., Fernandes, J. & Garvey, W. (2003) *Diabetes* 52, A330 (abstr).

www.pnas.org/cgi/doi/10.1073/pnas.0405278101

insulin resistance (22), and a major contributor of plasma PAI-1 in the obese (23).

Materials and Methods

Reagents. Methyl-β-cyclodextrin (MBCD) and filipin III were obtained from Sigma. Monoclonal antibodies against E2F1 (KH-95) and E2F2 (TFE-25) and rabbit polyclonal antibodies against E2F3 (C-18), E2F4 (C-20), E2F5 (C-20), pRB (M-153), p130 (C-20), p107 (C-18), IRS-1 (C-20), Erk, and PAI-1 (H-135) were from Santa Cruz Biotechnology. Rabbit polyclonal antibodies against phospho-pRB (Ser-795) and phospho-Erk were from Cell Signaling Technology (Beverly, MA). Rabbit polyclonal antibodies against Shc and phospho-tyrosine (G410) were from Transduction Laboratories (Lexington, KY). Sheep polyclonal antibody against PAI-1 was from American Diagnostics (Greenwich, CT). All reagents for real-time PCR were from Applied Biosystems. The oligonucleotide E2pro, the sequence of which corresponded to nucleotides −72 to −32 of the adenovirus E2 promoter and contained E2F-binding sites, had the following sequence (only the upper strand is given) and was used for gel-shift assays: 5′-GAT CAG TTT TCG CGC TTA AAT TTG AGA AAG GGC GCG AAA CTA G-3′.

Adipocyte Differentiation. 3T3-L1 preadipocytes were cultured in DMEM containing 10% FCS, and 2 days after cells reached confluency, the medium was changed to DMEM containing 10% FCS, 10 μg/ml insulin, 1 μM dexamethasone, and 0.5 mM isobutylmethylxanthine. Two to three days later, this medium was replaced with DMEM supplemented only with 10 μg/ml insulin, and cells were kept for 2 days. The medium was then replaced with DMEM containing 10% FCS every 2 days. The cells were serum-starved overnight before experiments.

Immunoprecipitation and Western Blotting. Immunoprecipitation and Western blotting were performed as described (24).

Glucose Uptake Assay. Measurements of 2-deoxyglucose uptake into adipocytes were carried out as described (25).

RNA Isolation and Northern Blot Analysis. Total RNA (12 μg) was isolated and subjected to Northern blot analysis as described (26). The cDNA clone for mouse PAI-1 was provided by A. Riccio (University of Naples, Naples).

Quantitative Real-Time PCR. One microgram of total RNA was reverse transcribed and 1 μl of RT reaction was added to 24 μl of PAI-1 PCR reaction (1× universal master mix/900 nM forward primer [5′-CCTGGCCGACTTCACAAGTC-3′]/900 nM reverse primer [5′-TTGCAGTGCCTGTGCTACAGA-3′]/200 nM TaqMan probe [5′-FAM-TCCGACCAAGAGC-MGB-3′]). Thermal cycling was done as follows: 50°C for 2 min, followed by 95°C for 10 min and then 45 cycles of 95°C for 1 min and 60°C for 1 min. The fluorophor dyes for the PAI-1 probe and 18S rRNA (internal control) probe were 6-carboxyfluorescein and VIC, respectively. The quencher in both probes was tetramethylrhodamine. The reaction was carried out in an ABI Prism 7700. The output raw data were normalized with internal control and statistically analyzed by using MS EXCEL (Microsoft).

Small Interfering RNA (siRNA) Nucleofection. siRNA used for targeting caveolin-1 mRNA has the following sequence: sense, 5′-GAGCUUCCUGAUUGAGAUU-3′ and antisense, 5′-AAUCUCAAUCAGGAAGCUC-3′. Control siRNA sequences: sense, 5′-GUACCUGACUAGUCGCAGAAG-3′ and antisense, 5′-UCUGCGACUAGUCAGGUACGG-3′. These sequences contain 3′ UU overhangs. Specificities of these sequences were confirmed by performing a BLAST search against the GenBank/European Molecular Biology Laboratory database. Each siRNA (final concentration 1 μM) was mixed with NIH 3T3 cells overexpressing the human IR (NIH-IR) cell suspension (2×10^6 cells in 0.1 ml of buffer-T/transfection), transferred to a 2-mm electroporation cuvette, and electroporated by using an Amaxa Nucleofector (Amaxa, Cologne, Germany) by using the program A-23. After electroporation, cells were immediately transferred to 1 ml of growth medium, and cultured in six-well plates at 37°C until analysis.

p70 Ribosomal S6 Kinase 1 (S6K1)$^{-/-}$ and PKBβ$^{-/-}$ Mice. PKBα knockout mice were generated as described (27). S6K1 knockout mice (28) were kindly provided by G. Thomas (Friedrich Miescher Institute). The S6K1$^{-/-}$ mice and their wild-type counterparts were fed with high-fat diet for 5–6 months (required for hyperactivity of PI3K pathway) before their blood was taken by using tail punctures. PKBα$^{-/-}$ mice were fed with a normal chow diet.

Cell-Penetrating Peptide Treatment. The sequence of the interfering peptide of 18-aa length was derived from the pRB-binding region of E2F1 (amino acids 402–419: LDYHFGLEEGEGIRDLFD) (29). A control peptide with the same amino acid composition, GEELEGFHDGLLDFDIR, was prepared by randomly shuffling the sequence of this peptide. Cell-penetrating peptides were prepared by coupling these peptides to the carboxy terminal of the cell-penetrating region of the HIV tat protein (amino acid 47–57: RRRQRRKKR) (30) via hinge peptide G. Differentiated adipocytes were separated from undifferentiated cells by using a Percoll density gradient as described (31) with a slight modification. Adipocytes were pretreated with collagenase (2 mg/ml) for 30 min, centrifuged at 1,500 rpm (Sorvall H4000,

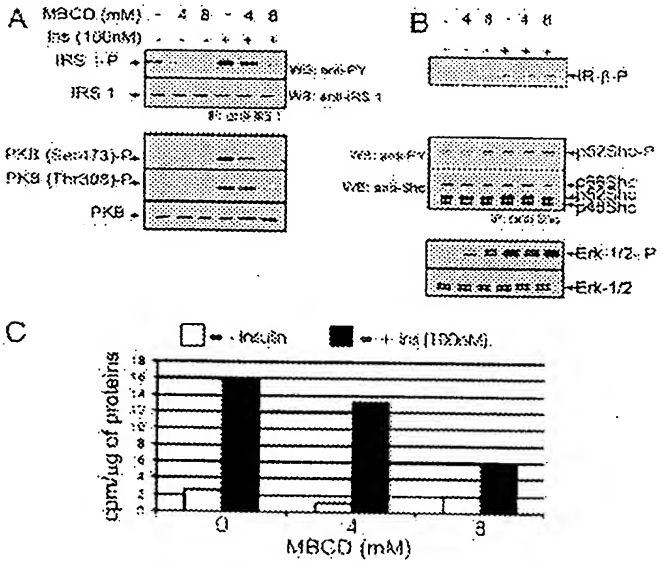

Fig. 1. Effect of cholesterol depletion on insulin signaling. 3T3L1 adipocytes were treated with 0, 4, or 8 mM MBCD for 40 min, followed by insulin treatment (100 nM) for 10 min, and then whole-cell extracts were prepared. The cell lysates were fractionated by SDS/PAGE, followed by Western blotting analysis using the specific antibodies indicated. For the analysis of IRS-1 and Shc, the lysates were first immunoprecipitated by using IRS-1 and Shc antibodies, respectively, before Western blotting. (*A*) Analysis of PKB and IRS-1, molecules involved in the metabolic signal pathway. (*B*) Analysis of the IR (IR) and its mitogenic signal transducers Shc and Erk. (*C*) Effect of MBCD on insulin-induced glucose uptake. Adipocytes were treated similarly as above and then subjected to a glucose uptake assay. All data shown here are representative of at least three independent experiments.

CELL BIOLOGY

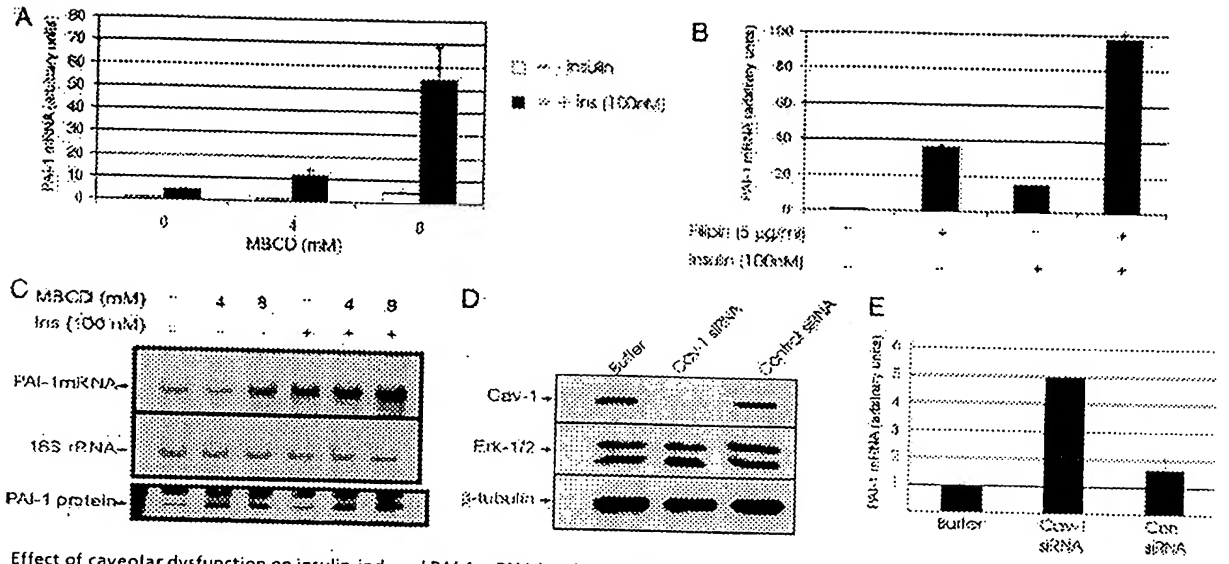

Fig. 2. Effect of caveolar dysfunction on insulin-induced PAI-1 mRNA levels. (*A*) Effect of MBCD on insulin-induced PAI-1 mRNA levels. 3T3L1 adipocytes were treated with 0, 4, or 8 mM MBCD for 40 min, with or without subsequent insulin treatment (100 nM) for 2 h. The total RNA was prepared and PAI-1 mRNA levels were measured by using real-time PCR with 18S rRNA as an internal control. (*B*) Effect of filipin on insulin-induced PAI-1 mRNA levels. Adipocytes were treated with filipin (5 μg/ml) for 40 min, with or without subsequent 2 h insulin (100 nM) treatment. Total RNA was analyzed as above. (*C*) Northern and Western blotting analysis. The same RNA samples used in *A* were subjected to Northern blot hybridization analysis for PAI-1 mRNA levels. For the analysis of PAI-1 protein levels, cells were treated with 0, 4, or 8 mM MBCD for 40 min, followed by insulin (100 nM) treatment for 6 h. Then, PAI-1 protein was immunoprecipitated from the conditioned media (because PAI-1 is a secreted protein) by using protein-G beads coupled to sheep anti-PAI-1 antibodies, and analyzed by Western blotting by using rabbit anti-PAI-1 antibodies. (*D* and *E*) Effects of caveolin down-regulation. NIH-IR cells were electroporated by using buffer without siRNA or with Cav-1 or control siRNA. After 24 h, the cells were treated with insulin (100 nM) for 2 h. Protein levels of caveolin-1, Erk, and β-tubulin (*D*) and mRNA levels of PAI-1 (*E*) were examined by Western blotting and RT-PCR, respectively.

Sorvall) for 5 min at 4°C, and mixed with Percoll solution (1.025 g/ml) to form a homogenous suspension. The cell suspension was then layered on preformed Percoll solution (1.035 g/ml) and centrifuged at 3,000 rpm (Sorvall H4000, Sorvall) for 20 min at 4°C. The cells collected from the upper layer were resuspended in media and reseeded for the experiment. The penetrating peptide was added to cells, incubated for 16 h, and then subjected to various treatments.

Nuclear Extracts and Electromobility-Shift Assays. Nuclear extracts (5 μg) were first incubated at room temperature for 15 min in 20 μl of binding reaction mixture containing 50 mM KCl, 20 mM Hepes (pH 7.9), 0.2 mM EDTA, 6% glycerol, 0.5% Ficoll 400, 1 μg of salmon sperm DNA, 6 μg of BSA, and 1 mM DTT with or without penetrating peptide and antibodies, followed by a further 15-min incubation after addition of 0.3 ng of radiolabeled oligonucleotide probes. Oligonucleotide probes were radiolabeled by using *Escherichia coli* polynucleotide kinase and [γ-^{32}P]ATP. Aliquots (5 μl) of reaction mixture were separated in a 4.5% polyacrylamide gel run in 0.25× TBE buffer (90 mM Tris/64.6 mM boric acid/2.5 mM EDTA, pH 8.3) at room temperature. The gel was dried and analyzed in a PhosphorImager.

Results

Perturbation of Caveolar Function Mimics Insulin Resistance in 3T3L1 Adipocytes. To find out whether caveolar dysfunction can cause insulin resistance, we perturbed the integrity of caveolar microdomains and examined the subsequent effects on insulin signaling. Cholesterol depletion using MBCD, a reagent widely used to perturb the structural integrity of caveolae, was used. MBCD pretreatment dose-dependently inhibited insulin-induced IRS-1 phosphorylation, PKB phosphorylation (Fig. 1*A*), and 2-deoxyglucose uptake (Fig. 1*C*). On the other hand, MBCD pretreatment did not affect insulin-induced phosphorylation of the β-subunit of the IR, Shc, or Erk (Fig. 1*B*). MBCD treatment alone (in the absence of insulin) was also found to increase the phosphorylation of p52 Shc and Erk-1/2, although to a lesser extent (Fig. 1*B*).

Induction of Insulin Resistance Leads to Concomitant Increase in PAI-1 Gene Expression. To determine whether MBCD-induced insulin resistance leads to the up-regulation of insulin-induced PAI-1 gene expression, we measured PAI-1 mRNA levels after insulin treatment with or without MBCD pretreatment. Results from both real-time PCR (Fig. 2*A*) and Northern blot hybridization (Fig. 2*C*) show that MBCD dose-dependently increased insulin-induced PAI-1 levels. To find out whether this increase at the mRNA level is reflected at the protein level, PAI-1 protein levels were measured in the media. Corresponding to the mRNA levels, insulin-induced PAI-1 protein levels were dose-dependently up-regulated by MBCD treatment. Filipin, a structurally distinct sterol-binding compound, also augmented the insulin-induced PAI-1 levels (Fig. 2*B*), suggesting that the observed MBCD effects were through perturbation of caveolae function per se. Fig. 2 *A* and *B* clearly show that the effect of cholesterol depletion synergistically up-regulated insulin-induced PAI-1 gene expression. To ascertain that the up-regulation of PAI-1 observed here is due to caveolar dysfunction and not due to an unspecific effect of cholesterol depletion, we depleted the caveolin-1 protein using siRNA directed against caveolin-1 mRNA. In this experiment, NIH-IR were used instead of adipocytes, which proved difficult to transfect efficiently with siRNA. NIH-IR cells were chosen as the suitable alternative to adipocytes, because they are insulin-sensitive, rich in caveolae, share a common cell lineage with adipocytes, and can be differentiated into adipocytes (32). This siRNA showed specific effects, because it significantly lowered the caveolin-1 protein levels but did not affect the levels of other proteins such as Erk and β-tubulin (Fig. 2*D*). Furthermore, control siRNA had no effect on any of these proteins. Caveolin-1 siRNA treatment

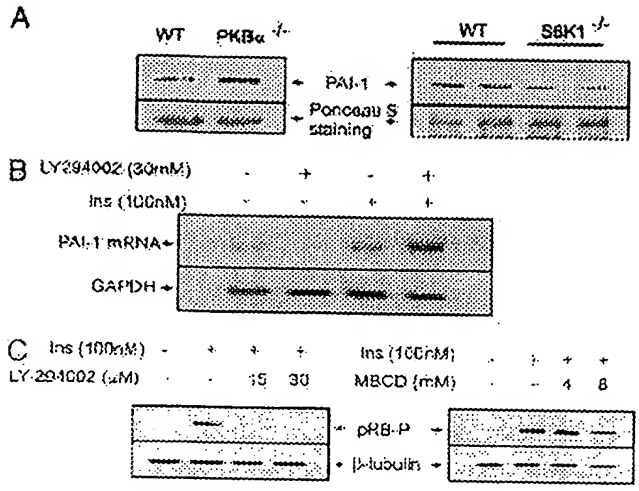

Fig. 3. The role of the PI3K pathway in PAI-1 gene expression. (*A*) Serum PAI-1 levels of PKB$\alpha^{-/-}$, S6K1$^{-/-}$ mice, and their wild-type counterparts were analyzed by PAI-1 immunoprecipitation followed by Western blotting. The membranes were stained with Ponceau S for loading control. (*B*) 3T3L1 adipocytes were treated with LY294002 (30 μM) for 45 min, followed by insulin (100 nM) for 2 h. Total RNA was prepared and analyzed for levels of PAI-1 and GAPDH (loading control) mRNAs by Northern blot hybridization. (*C*) 3T3L1 adipocytes were treated with increasing concentrations of either LY294002 or MBCD for 45 min, followed by insulin (100 nM) for 2 h, and the phosphorylation status of pRB and the protein levels of β-tubulin (loading control) were measured by Western blotting.

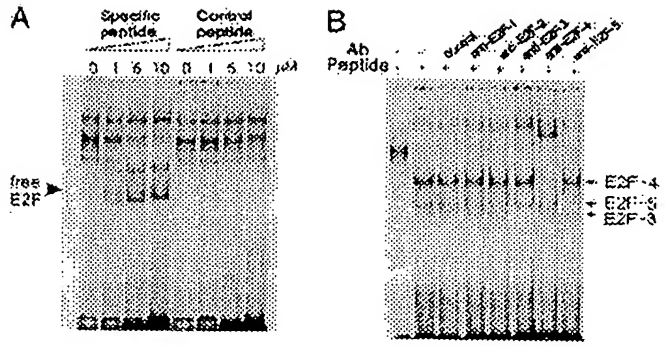

Fig. 4. Effect of cell-penetrating interfering peptide on free E2F levels. (*A*) In DNA gel-shift assays using ^{32}P-labeled E2pro oligonucleotide and nuclear extracts from adipocytes, cell-penetrating peptide (specific and control peptides) was added to binding reactions at increasing concentrations. (*B*) Nuclear extracts (day 8) were preincubated with the cell-penetrating interfering peptide together with specific antibodies against different E2F members for 15 min and then analyzed for E2F DNA-binding activity by gel-shift assays as above.

enhanced the levels of insulin-induced PAI-1 5-fold, whereas control siRNA had no significant effect (Fig. 2*E*).

Impairment of PI3K Pathway Leads to Transcriptional Up-Regulation of PAI-1. To see whether the up-regulation of insulin-induced PAI-1 by caveolar dysfunction was a direct consequence of impaired metabolic signaling (PI3K pathway), we examined the levels of plasma PAI-1 in two different mouse models that are hallmarked by augmented (S6K1$^{-/-}$) and attenuated (PKB$\alpha^{-/-}$) metabolic signaling. Activated S6K1 phosphorylates IRS-1 at serine residues and suppresses its tyrosine phosphorylation by IR. Thus, deletion of S6K1 augments PI3K signaling in these mice (33). On the other hand, PKB is a critical mediator of PI3K signaling. Thus, deletion of PKB would attenuate the PI3K signal pathway. As shown in Fig. 3*A*, plasma PAI-1 levels were up-regulated in PKB$\alpha^{-/-}$ mice, whereas they were down-regulated in S6K1$^{-/-}$ mice. The negative regulation of PAI-1 gene expression by the PI3K pathway was further confirmed in adipocyte cell culture, where PI3K inhibitor (LY294002) enhanced insulin-induced PAI-1 mRNA levels (Fig. 3*B*). Treatment with LY294002 and MBCD, both shown to inhibit the PI3K pathway, dose-dependently inhibited insulin-induced pRB phosphorylation (Fig. 3*C*), thus providing a possible explanation of why PI3K pathway activation leads to the down-regulation of PAI-1 gene expression (see below).

Disruption of pRB–E2F Interaction Using a Cell-Penetrating Peptide. Hypophosphorylated pRB is bound to E2F forming an inactive complex, whereas hyperphosphorylation of pRB leads to the release of free E2F (18). We have previously shown that overexpression of E2F isoforms can down-regulate PAI-1 gene expression (19). It has also been shown that active pRB, which can bind to E2F, reverses this down-regulation (26). Taken together, these results suggest that free E2F acts as a transcriptional repressor of the PAI-1 gene. We have observed that pRB phosphorylation is increased, whereas E2F-1 protein levels are reduced during adipogenesis (data not shown), suggesting that E2F activity (corresponding to free E2F) may be compromised in differentiated adipocytes. To restore the potential of E2F-mediated transcriptional repression of the PAI-1 gene in adipocytes, we sought to release free E2F by disrupting the E2F–pRB complex using an interfering peptide that corresponds to amino acids 402–419 of E2F1, the domain interacting with the pocket proteins (29). A BLAST search revealed that this domain is fairly conserved among members of the E2F family (excluding E2F-6) and, therefore, the peptide that we designed may disrupt the pocket protein–E2F interaction in general. As a control, we used a peptide with a randomly shuffled sequence. To render these peptides cell-penetrable, an HIV-1 Tat-derived peptide sequence was tagged to these peptides (30). The avidity of these peptides to disrupt the E2F–pRB complex was confirmed by DNA gel-shift assays using adipocyte nuclear extracts and a radioactive oligonucleotide, the sequence of which corresponds to the E2F-binding site of the adenovirus E2 promoter. As shown in Fig. 4*A*, DNA–protein complexes shifted to low-molecular-weight forms when increasing concentrations of the specific peptide were added to binding mixtures; the control peptide had no effect. Supershift assays using specific antibodies against E2F1–5 revealed that the main isoforms in the freed E2F fractions were E2F3, -4, and -5 (Fig. 4*B*). These peptides thus serve as an effective tool to disrupt endogenous E2F–pRB interactions.

Elevation of PAI-1 Levels in Insulin Resistance Is Suppressed by the Cell-Penetrating Peptide. To examine whether interfering peptide treatment can compromise induction of PAI-1 by hyperinsulinemia and insulin resistance, we performed the following experiments. Adipocytes were prepared according to *Materials and Methods* and were treated with either the specific or control peptide for 12 h followed by 1 μM insulin for 2 h. As shown in Fig. 5*A*, the specific peptide, but not the control peptide, suppressed both basal and insulin-induced PAI-1 levels in a dose-dependent manner, the latter being more potently affected (Fig. 5*A*). Furthermore, the specific peptide also suppressed PAI-1 expression that was up-regulated by MBCD-induced insulin resistance (Fig. 5*B*). Again, the control peptide had no effect.

Discussion

Obesity is characterized by increased adipocyte mass and altered adipocyte physiology. These traits contribute to the progression

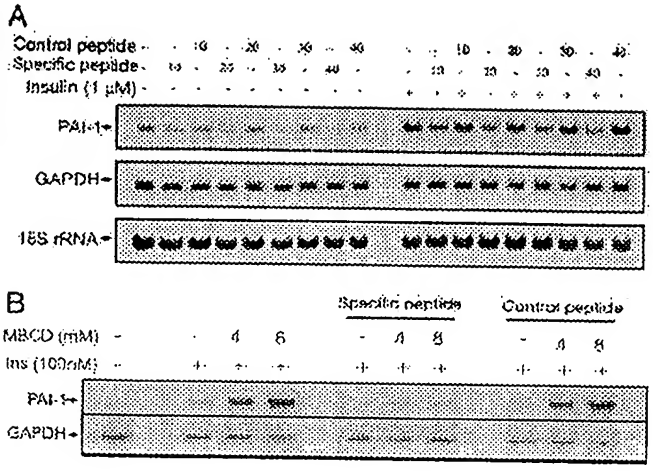

Fig. 5. Effect of cell-penetrating interfering peptide on PAI-1 mRNA levels. (*A*) Dose-response of the peptides. 3T3L1 adipocytes (day 8) were treated with increasing concentrations (0–40 μM) of either specific or control peptide for 6 h, followed by treatment with or without 1 μM insulin for 2 h. Total RNA was prepared, and levels of PAI-1 and GAPDH (loading control) mRNAs were measured by Northern blot hybridization. Ribosomal RNAs were stained with methylene blue to serve as an additional control for equal loading and blotting. (*B*) Effect of the peptides on PAI-1 mRNA levels, which are elevated under insulin-resistant conditions. Cells were serum-starved and then treated with 40 μM of specific or control peptides for 12 h. Cells were then treated with MBCD for 40 min, followed by insulin (100 nM) for 2 h. Total RNA was prepared and analyzed for PAI-1 mRNA as above.

from obesity to insulin resistance (34). Reductions in plasma membrane cholesterol and protein levels of caveolin-1/3 are associated with adipocyte hypertrophy and obesity, respectively (5, 6). It is thought that this could lead to caveolar dysfunction, because plasma membrane cholesterol and caveolin are essential for the structural and functional integrity of caveolae (6, 7). To study the acute effects of caveolar dysfunction in adipocytes, we used cholesterol-scavenging reagents, such as MBCD, which are known to perturb caveolae in adipocytes (35). Kinetic studies have suggested that the vast majority of cholesterol scavenged by cyclodextrins is from the plasma membrane (36), where >90% of cellular cholesterol is known to reside (37). Treatment with MBCD did not affect insulin-induced tyrosine phosphorylation of the IR and its downstream mitogenic signaling, but impaired the IRS-PKB signal pathway that leads to glucose uptake (Fig. 1 *A* and *B*). This suggests that cholesterol depletion and, presumably, consequent caveolar dysfunction would lead to insulin resistance. Consistently, it was recently reported that caveolin-1$^{-/-}$ and caveolin-3$^{-/-}$ mice, both known to have a dramatic reduction in caveolae, exhibit insulin resistance (38, 39). Moreover, in adipocytes treated with TNF-α, the IR accumulated less in the detergent-insoluble low-density membrane fractions (microdomains) and shifted to the high-density fractions, suggesting a translocation of IR from caveolar to noncaveolar fractions (40). TNF-α is a potent inducer of insulin resistance (41) and PAI-1 gene expression (42). It is chronically elevated in conditions of obesity and is a major culprit in the pathogenesis of obesity-driven insulin resistance (41). Thus, denying the caveolar platform for IR signaling could be a plausible mechanism through which obesity per se and its secondary effectors elicit insulin resistance. Our hypothesis warrants further investigations into the structural and functional integrity of caveolae in obese and T2DM patients.

Treatment of adipocytes with two structurally distinct cholesterol-depleting reagents (MBCD and filipin) leads to up-regulation of insulin-induced expression of PAI-1 mRNA and protein levels (Fig. 2 *A–C*). Similar up-regulation is also obtained in NIH-IR cells after RNAi-mediated caveolin-1 down-regulation (Fig. 2*E*). Thus, perturbation of caveolae by depleting their integral components, either cholesterol or caveolin-1, leads to significant up-regulation of insulin-induced PAI-1 gene expression. MBCD alone induces PAI-1 mRNA to a certain extent (Fig. 2), but this level of induction can be explained by a slight activation of Erk, because Erk has been reported to up-regulate the PAI-1 gene by activating the AP-1 transcription factor (43). However, the MBCD-mediated synergistic increase in insulin-induced PAI-1 gene expression cannot be explained by Erk activation, because the extent of insulin-induced Erk phosphorylation (Fig. 1*B*) was not affected by MBCD cotreatment. We therefore postulate an alternative mechanism for the up-regulation of insulin-induced PAI-1 gene expression mediated by caveolar dysfunction (see below).

Insulin-induced PAI-1 mRNA levels are augmented by treatment with a specific PI3K inhibitor, suggesting that the PI3K pathway inhibits PAI-1 gene expression (Fig. 3*B*). We show that the level of serum PAI-1 is increased in PKBα$^{-/-}$ mice, whereas it is reduced in S6K1$^{-/-}$ mice (Fig. 3*A*). The whole blood protein concentration in both PKBα and S6K1$^{-/-}$ is similar to that of their wild-type littermates. These results suggest that the functional state of the PI3K pathway plays an important role in the regulation of PAI-1 gene expression.

There are several reports of the PI3K pathway regulating pRB–E2F interactions in a cell-type-independent manner. Activation of PKB by inhibition of its phosphatases reduced the pRB phosphorylation and E2F1 release in C141 cells (44). In T lymphocytes, expression of active PKB is sufficient to induce E2F activity (45). In C33A cells, both wortmannin (PI3K inhibitor) treatment and overexpression of PTEN (a negative regulator of the PI3K-PKB pathway) inhibited pRB phosphorylation, and this was reversed by coexpression of a catalytically active subunit of PI3K (46). In NIH 3T3 fibroblasts, epidermal growth factor-induced pRB phosphorylation and hence G_1 to S phase cell cycle progression were inhibited by both LY294002 and wortmannin (47). In agreement with the finding of Usui *et al.* (17), we show that LY294002 inhibits insulin-induced phosphorylation of pRB in 3T3L1 adipocytes. MBCD also shows similar effects (Fig. 3*C*), implying that impaired metabolic signaling, characteristic of insulin resistance, may reduce the phosphorylation of pRB. Hypophosphorylated pRB is known to bind E2F1–3 proteins and inhibits their activity either by directly binding to and masking the transactivation domain of E2F or by recruiting histone deacetylases (18). Reduction in pRB phosphorylation, therefore, will result in the reduction of free E2F levels. We have previously shown (26) that free E2F can act as a repressor of PAI-1 gene expression in a variety of cell lines, including U2OS, T98G, SAOS2, LLC-PK1, and MEF cells, suggesting that the E2F-mediated negative regulation of PAI-1 gene expression is a general phenomenon independent of cell type. These observations taken together, we propose that the PI3K pathway in insulin signaling negatively regulates the PAI-1 gene through phosphorylation of pRB and subsequent release of free E2F. This, in essence, is suggestive of differential regulation of PAI-1 gene expression by insulin; positive regulation through the mitogenic pathway, and negative regulation through the metabolic pathway (see Fig. 6, which is published as supporting information on the PNAS web site). The compromised metabolic pathway may explain why insulin-induced PAI-1 levels are up-regulated in states of caveolar dysfunction.

It is widely accepted that PAI-1 levels are raised in conditions of obesity and insulin resistance (9) and play a key role in the development of cardiovascular complications in these patients. Recent studies show that PAI-1 knockout mice are resistant to high-fat-diet-induced obesity and insulin resistance, although the underlying molecular mechanisms are not well understood (48,

49). In line with the data from Vuori *et al.* (50) showing that vitronectin–$\alpha_v\beta_3$ integrin interaction facilitates insulin-induced IRS-1 activation, we had earlier proposed a model in which PAI-1 can induce insulin resistance by binding to vitronectin and inhibiting its interaction with $\alpha_v\beta_3$ integrin (51). This suggests that PAI-1 can be a cause as well as a consequence of insulin resistance, and reducing its levels may offer immense therapeutic value. Both basal and insulin-induced PAI-1 levels could be dramatically reduced by treating adipocytes with a cell-penetrating peptide that physically disrupts the pRB–E2F interaction (Fig. 5*A*). Furthermore, the interfering peptide was also able to suppress the elevation of PAI-1 mRNA levels in insulin-resistant adipocytes (Fig. 5*B*). These results strengthen our hypothesis that insulin negatively suppresses PAI-1 gene expression through E2F proteins.

Conclusion

We have demonstrated that caveolar dysfunction leads to the selective impairment of the PI3K pathway in adipocytes. This compromises E2F-mediated suppression of PAI-1 gene expression, resulting in the concomitant up-regulation of PAI-1 levels. Our work thus establishes a direct link between impaired PI3K pathway and elevated PAI-1 gene expression, both characteristics of insulin-resistant conditions. We also propose a pharmacological paradigm of disrupting pRB–E2F interaction to suppress PAI-1 levels that are elevated during insulin resistance (see Fig. 6). Recently, the crystal structure of E2F bound to pRB was solved (52), and this should facilitate the development of small molecule inhibitors of E2F–pRB interaction.

We are grateful to Sung Hee Um and Francesca Frigerio (Friedrich Miescher Institute) for help with the S6K1$^{-/-}$ mice and Marco Falasca (University College London, London) for the NIH-IR cells. We thank Timothy Garvey (Medical University of South Carolina, Charleston, SC), Wilhelm Krek (Eidgenössische Technische Hochschule, Zurich) and Sandra Kleiner (Friedrich Miescher Institute) for helpful discussions. Derek Brazil (Conway Institute, Dublin) and Hoanh Tran (Medical Research Council–Laboratory of Molecular Biology, Cambridge, U.K.) are duly acknowledged for critical reading of the manuscript. This work was partly supported by the Roche Research Foundation (fellowship to K.H.).

1. Saltiel, A. R. & Kahn, C. R. (2001) *Nature* **414**, 799–806.
2. Shao, J., Yamashita, H., Qiao, L. & Friedman, J. E. (2000) *J. Endocrinol.* **167**, 107–115.
3. Cusi, K., Maezono, K., Osman, A., Pendergrass, M., Patti, M. E., Pratipanawatr, T., DeFronzo, R. A., Kahn, C. R. & Mandarino, L. J. (2000) *J. Clin. Invest.* **105**, 311–320.
4. Krook, A., Bjornholm, M., Galuska, D., Jiang, X. J., Fahlman, R., Myers, M. G., Jr., Wallberg-Henriksson, H. & Zierath, J. R. (2000) *Diabetes* **49**, 284–292.
5. Le Lay, S., Krief, S., Farnier, C., Lefrere, I., Le Liepvre, X., Bazin, R., Ferre, P. & Dugail, I. (2001) *J. Biol. Chem.* **276**, 16904–16910.
6. Dreja, K., Voldstedlund, M., Vinten, J., Tranum-Jensen, J., Hellstrand, P. & Sward, K. (2002) *Arterioscler. Thromb. Vasc. Biol.* **22**, 1267–1272.
7. Drab, M., Verkade, P., Elger, M., Kasper, M., Lohn, M., Lauterbach, B., Menne, J., Lindschau, C., Mende, F., Luft, F. C., *et al.* (2001) *Science* **293**, 2449–2452.
8. Anderson, R. G. (1998) *Annu. Rev. Biochem.* **67**, 199–225.
9. McGill, J. B., Schneider, D. J., Arfken, C. L., Lucore, C. L. & Sobel, B. E. (1994) *Diabetes* **43**, 104–109.
10. Eddy, A. A. (2002) *Am. J. Physiol.* **283**, F209–F220.
11. Lambert, V., Munaut, C., Noel, A., Frankenne, F., Bajou, K., Gerard, R., Carmeliet, P., Defresne, M. P., Foidart, J. M. & Rakic, J. M. (2001) *FASEB J.* **15**, 1021–1027.
12. Vaughan, D. E. (2003) in *Diabetes mellitus*, eds. Porte, D., Sherwin, R. S. & Baron, A. (McGraw–Hill, New York), pp. 175–178.
13. Kaikita, K., Fogo, A. B., Ma, L., Schoenhard, J. A., Brown, N. J. & Vaughan, D. E. (2001) *Circulation* **104**, 839–844.
14. Lyon, C. J. & Hsueh, W. A. (2003) *Am. J. Med.* **115 Suppl 8A**, 62S–68S.
15. Samad, F., Pandey, M., Bell, P. A. & Loskutoff, D. J. (2000) *Mol. Med.* **6**, 680–692.
16. Griffiths, M. R., Black, E. J., Culbert, A. A., Dickens, M., Shaw, P. E., Gillespie, D. A. & Tavare, J. M. (1998) *Biochem. J.* **335**, 19–26.
17. Usui, I., Haruta, T., Iwata, M., Takano, A., Uno, T., Kawahara, J., Ueno, E., Sasaoka, T. & Kobayashi, M. (2000) *Biochem. Biophys. Res. Commun.* **275**, 115–120.
18. Trimarchi, J. M. & Lees, J. A. (2002) *Nat. Rev. Mol. Cell. Biol.* **3**, 11–20.
19. Koziczak, M., Krek, W. & Nagamine, Y. (2000) *Mol. Cell. Biol.* **20**, 2014–2022.
20. Parton, R. G. (2003) *Nat. Rev. Mol. Cell. Biol.* **4**, 162–167.
21. White, M. F. & Kahn, C. R. (1994) *J. Biol. Chem.* **269**, 1–4.
22. Hotamisligil, G. S. (2000) *Int. J. Obes. Relat. Metab. Disord.* **24 Suppl 4**, S23–27.
23. Mavri, A., Alessi, M. C., Bastelica, D., Geel-Georgelin, O., Fina, F., Sentocnik, J. T., Stegnar, M. & Juhan-Vague, I. (2001) *Diabetologia* **44**, 2025–2031.
24. Faisal, A., Kleiner, S. & Nagamine, Y. (2004) *J. Biol. Chem.* **279**, 3202–3211.
25. Sweeney, G., Somwar, R., Ramlal, T., Volchuk, A., Ueyama, A. & Klip, A. (1999) *J. Biol. Chem.* **274**, 10071–10078.
26. Koziczak, M., Muller, H., Helin, K. & Nagamine, Y. (2001) *Eur. J. Biochem.* **268**, 4969–4978.
27. Yang, Z. Z., Tschopp, O., Hemmings-Mieszczak, M., Feng, J., Brodbeck, D., Perentes, E. & Hemmings, B. A. (2003) *J. Biol. Chem.* **278**, 32124–32131.
28. Shima, H., Pende, M., Chen, Y., Fumagalli, S., Thomas, G. & Kozma, S. C. (1998) *EMBO J.* **17**, 6649–6659.
29. Helin, K., Lees, J. A., Vidal, M., Dyson, N., Harlow, E. & Fattaey, A. (1992) *Cell* **70**, 337–350.
30. Vives, E. & Lebleu, B. (2002) in *Cell-Penetrating Peptides*, ed. Langel, U. (CRC, Boca Raton, FL), Vol. 1, pp. 3–23.
31. Ramsay, T. G., Hausman, G. J. & Martin, R. J. (1987) *J. Anim. Sci.* **64**, 735–744.
32. Hwang, C. S., Loftus, T. M., Mandrup, S. & Lane, M. D. (1997) *Annu. Rev. Cell Dev. Biol.* **13**, 231–259.
33. Um, S. H., Frigerio, F., Watanabe, M., Picard, F., Joaquin, M., Sticker, M., Fumagalli, S., Allegrini, P. R., Kozma, S. C., Auwerx, J. & Thomas, G. (2004) *Nature* **431**, 200–205.
34. Kahn, S. E. & Porte, D. (2003) in *Ellenberg and Rifkin's Diabetes Mellitus*, eds. Porte, D., Sherwin, R. S. & Baron, A. (McGraw–Hill, New York), pp. 331–367.
35. Gustavsson, J., Parpal, S., Karlsson, M., Ramsing, C., Thorn, H., Borg, M., Lindroth, M., Peterson, K. H., Magnusson, K. E. & Stralfors, P. (1999) *FASEB J.* **13**, 1961–1971.
36. Yancey, P. G., Rodrigueza, W. V., Kilsdonk, E. P., Stoudt, G. W., Johnson, W. J., Phillips, M. C. & Rothblat, G. H. (1996) *J. Biol. Chem.* **271**, 16026–16034.
37. Lange, Y., Swaisgood, M. H., Ramos, B. V. & Steck, T. L. (1989) *J. Biol. Chem.* **264**, 3786–3793.
38. Cohen, A. W., Razani, B., Wang, X. B., Combs, T. P., Williams, T. M., Scherer, P. E. & Lisanti, M. P. (2003) *Am. J. Physiol.* **285**, C222–C235.
39. Oshikawa, J., Otsu, K., Toya, Y., Tsunematsu, T., Hankins, R., Kawabe, J., Minamisawa, S., Umemura, S., Hagiwara, Y. & Ishikawa, Y. (2004) *Proc. Natl. Acad. Sci. USA* **101**, 12670–12675.
40. Kabayama, K., Sato, T., Kitamura, F., Uemura, S., Kang, B. W., Igarashi, Y. & Inokuchi, J. I. (2004) *Glycobiology*, in press.
41. Hotamisligil, G. S., Shargill, N. S. & Spiegelman, B. M. (1993) *Science* **259**, 87–91.
42. Samad, F., Uysal, K. T., Wiesbrock, S. M., Pandey, M., Hotamisligil, G. S. & Loskutoff, D. J. (1999) *Proc. Natl. Acad. Sci. USA* **96**, 6902–6907.
43. Hsueh, W. A. & Law, R. E. (1998) *Am. J. Med.* **105**, 4S–14S.
44. Zhang, Z., Gao, N., He, H., Huang, C., Luo, J. & Shi, X. (2004) *Mol. Cell Biochem.* **255**, 227–237.
45. Brennan, P., Babbage, J. W., Burgering, B. M., Groner, B., Reif, K. & Cantrell, D. A. (1997) *Immunity* **7**, 679–689.
46. Paramio, J. M., Navarro, M., Segrelles, C., Gomez-Casero, E. & Jorcano, J. L. (1999) *Oncogene* **18**, 7462–7468.
47. Takuwa, N., Fukui, Y. & Takuwa, Y. (1999) *Mol. Cell. Biol.* **19**, 1346–1358.
48. Ma, L. J., Mao, S. L., Taylor, K. L., Kanjanabuch, T., Guan, Y., Zhang, Y., Brown, N. J., Swift, L. L., McGuinness, O. P., Wasserman, D. H., Vaughan, D. E. & Fogo, A. B. (2004) *Diabetes* **53**, 336–346.
49. Schafer, K., Fujisawa, K., Konstantinides, S. & Loskutoff, D. J. (2001) *FASEB J.* **15**, 1840–1842.
50. Vuori, K. & Ruoslahti, E. (1994) *Science* **266**, 1576–1578.
51. Lopez-Alemany, R., Redondo, J. M., Nagamine, Y. & Munoz-Canoves, P. (2003) *Eur. J. Biochem.* **270**, 814–821.
52. Xiao, B., Spencer, J., Clements, A., Ali-Khan, N., Mittnacht, S., Broceno, C., Burghammer, M., Perrakis, A., Marmorstein, R. & Gamblin, S. J. (2003) *Proc. Natl. Acad. Sci. USA* **100**, 2363–2368.

APPENDIX D

ANTISENSE AND NUCLEIC ACID DRUG DEVELOPMENT 12:411–418 (2002)

Brief Communication

The Effectiveness of Double-Stranded Short Inhibitory RNAs (siRNAs) May Depend on the Method of Transfection

D.K. WALTERS and D.F. JELINEK

ABSTRACT

RNA interference (RNAi) is a recently described powerful experimental tool that can cause sequence-specific gene silencing, thereby facilitating functional analysis of gene function. Consequently, we became interested in using RNAi to determine the function of aberrantly expressed ErbB3 in the KAS-6/1 human myeloma cell line. Despite the wealth of information available on the use of RNAi, dsRNA target design, and the transfection of dsRNA *in vitro*, little information is available for transfecting dsRNA into nonadherent cells from any species. In the present study, we report that gene silencing of ErbB3 was not observed in myeloma cells when dsRNA targeting ErbB3 was introduced using conventional transfection agents and protocols that have proved successful for several adherent cell lines. Silencing of ErbB3, however, was observed in T47D cells, an adherent breast carcinoma cell line, using the same transfection methods, indicating that our target sequence was functional for gene silencing of ErbB3. Interestingly, ErbB3 was silenced in myeloma cells when the dsRNA target was introduced by electroporation. Thus, our studies illustrate the striking dependence of dsRNA-mediated gene silencing in some cells on the methods of dsRNA transfection.

INTRODUCTION

RNA INTERFERENCE (RNAi), a phenomenon first discovered in *Caenorrhabditis elegans*, is a response to double-stranded RNA (dsRNA) that can cause sequence-specific gene silencing (Fire et al., 1998). At present, the mechanism of this phenomenon is not entirely understood, but current models propose the involvement of two distinct steps (Hutvagner and Zamore, 2002). The first, initiation step involves cellular uptake or input of long strands of dsRNA and the subsequent enzymatic digest of these strands into 21–23-nucleotide (nt) small interfering RNAs (siRNAs), which are often referred to as "guide RNAs" (reviewed in Hannon, 2002). In the second, effector step, the guide RNAs bind to the RNA-induced silencing complex (RISC), a nuclease complex proposed to have helicase activity, endonuclease activity, and homology searching activity (Hammond et al., 2001). Consequently, it is believed that the RISC complex is able to unwind the bound double-stranded guide RNA and then targets the homologous endogenous transcript via base pairing interactions. The endogenous transcript is subsequently cleaved by the RISC complex, resulting in downregulation or silencing of the gene.

The utility of this discovery for quickly and easily determining the function of a gene was immediately recognized and led to an examination of the ability of chemically synthesized siRNA duplexes to silence genes of interest. Indeed, several groups have now described successful results of specific gene silencing using siRNA

Department of Immunology, Tumor Biology Program, Mayo Graduate and Medical Schools, Mayo Clinic/Foundation, Rochester, MN 55905

duplexes (Dudley et al., 2002; Harborth et al., 2002; Li et al., 2002; Matuliene and Kuriyama, 2002; Tijsterman et al., 2002; Tuschl et al., 1999). Because of its early success, RNAi has become one of the hottest techniques since the invention of PCR. Consequently, we became interested in using RNAi to determine the function of aberrantly expressed ErbB3 in the KAS-6/1 human myeloma cell line. It is noteworthy, however, that successful use of RNAi in human cells, with only one exception (Wilda et al., 2002), has been accomplished using adherent cells. Our goal in this study was to further explore the feasibility of using RNAi in nonadherent human cells. In this report, we describe the methods that allowed us to use RNAi to silence ErbB3 in this cell line. Our results clearly illustrate that gene silencing using RNAi in this nonadherent cell line is critically dependent on the methods used to deliver RNA duplexes into the cell.

MATERIALS AND METHODS

Cell lines, culture medium, and reagents

The myeloma cell line, KAS-6/1, was derived from primary patient myeloma cells and has been described previously (Westendorf et al., 1996). This cell line was maintained in RPMI 1640 medium supplemented with 5% heat-inactivated fetal bovine serum (FBS), 100 U/ml penicillin G, 50 μg/ml gentamicin, 100 μg/ml streptomycin, 2 mmol/L glutamine, and 1 ng/ml interleukin-6 (IL-6) (Novartis Pharma AG, Basel, Switzerland). The breast adenocarcinoma cell line T47D was purchased from ATCC and maintained in DMEM supplemented with 10% heat-inactivated FBS, 100 U/ml penicillin G, 50 μg/ml gentamicin, 100 μg/ml streptomycin, and 2 mmol/L glutamine. Oligofectamine, Cellfectin, and DMRIE-C were purchased from Invitrogen (Carlsbad, CA).

Flow cytometry

To assess successful transfection of the fluorescein-labeled luciferase-specific siRNA duplex, cells were washed three times in ice-cold phosphate-buffered saline (PBS)/2% FBS to remove any surface-bound complex and then fixed in 1% paraformaldehyde. Immunofluorescence was detected using a FACScan flow cytometer (Becton Dickinson, Mountain View, CA). For measuring ErbB3 expression, 1×10^6 cells were incubated with an ErbB3 monoclonal antibody (mAb) (Neomarkers, Inc., Fremont, CA) for 30 minutes on ice in PBS/2% FBS, washed, and then incubated with phycoerythrin (PE)-conjugated goat antimouse IgG (Biosource International, Camarillo, CA) for another 30 minutes. Expression of gp130, insulin-like growth factor-I (IGF-IR), and VLA-4 (α4 integrin) was assessed via incubation with either PE-conjugated or FITC-conjugated receptor-specific Abs (Immunotech, Marseille, France; Molecular Probes, Eugene, OR; Serotec, Oxford, U.K., respectively) for 30 minutes on ice. Syndecan-1 expression was determined using an FITC-conjugated CD138 mAb (Serotec). All cells were then washed, fixed in 1% paraformaldehyde, and analyzed for immunofluorescence on a FACScan flow cytometer. To distinguish between intracellular and extracellular fluorescence, cells were incubated with or without a 0.2% solution of trypan blue for 5 minutes (Van Amersfoort and Van Strijp, 1994). Cells were washed twice with PBS and fixed as usual. The collected data were analyzed using WinMDI 2.5 software. The change in mean fluorescence intensity (ΔMFI) was calculated by dividing the MFI resulting from staining with the receptor-specific Ab by the MFI resulting from staining with the isotype control Ab.

Immunoprecipitation and immunoblotting

Following transfection, myeloma cells were cultured in RPMI supplemented with 10% FBS and IL-6, and breast carcinoma cells were cultured in DMEM medium supplemented with 10% bovine serum albumin (BSA) for 24, 48, 72, or 96 hours. Cells (5×10^6) were lysed in lysis buffer containing 50 mM Tris, pH 7.4, 150 mM NaCl, 1% NP-40, 0.5% DOC, 0.1% SDS, 1 mM EDTA, 15 mM sodium molybdate, 1 mM NaF, 10 μg/ml leupeptin, 10 μg/ml aprotinin, 10 μg/ml pepstatin, 2 mM Na_3VO_4, and 1 mM PMSF. Lysates were cleared of insoluble material by centrifugation for 10 minutes at 14,000 rpm. Whole cell lysate (75 μg) was diluted 1:1 with 2× SDS loading buffer, heated to 100°C for 5 minutes, resolved by SDS-PAGE, and transferred to Immobilon-P membranes (Millipore Corp., Bedford, MA) for immunoblotting. Membranes were blocked for 1 hour in 25 mM Tris-HCl, pH 7.2, 150 mM NaCl, and 0.2% Tween (TBST) supplemented with 2% BSA. Immunoblotting for ErbB3 was detected by a 1:1000 dilution of anti-ErbB3 mAb (Santa Cruz Biotechnology, Inc., Santa Cruz, CA), and horseradish peroxidase (HRP)-conjugated polyclonal antirabbit IgG (Amersham Pharmacia Biotech Inc., Piscataway, NJ) was used as the secondary at a dilution of 1:3000. Immunoreactive proteins were detected using an enhanced chemiluminescence (ECL) detection system (Super Signal, Pierce Biotechnology, Inc., Rockford, IL) and autoradiography.

Source of dsRNA molecules and transfection using Oligofectamine, Cellfectin, and DMRIE-C

The pGL2 siRNA duplex (target 5′-CGTACGCGGAATACTTCGA-3′), ErB3 siRNA duplex (target 5′-AACCAATACCAGACACTGTAC-3′), IGF-IR siRNA duplex (target 5′-CTACGCCCTGGTCATCTTC-3′), and survivin siRNA (target 5′-ACTGGACAGAGAAA-

GAGCC-3′) were synthesized and purchased from Dharmacon Research, Inc. (Lafayette, CO). The synthesis method was carried out according to the method described by Elbashir et al. (2001), in which a 21-nt sense and a 21-nt antisense strand are paired in a complementary manner. This pairing results in a target-specific 19-nt duplex region and a 2-nt overhang (dTdT for all the duplex RNAs used in this study) at the 3′-end. Duplexes labeled with fluorescein moieties were modified at the 5′-end of the sense strand. Transfection of these duplexes using Oligofectamine, Cellfectin, or DMRIE-C was carried out according to the procedure provided by Dharmacon (*www.dharmacon.com/siRNA.html*), which is also the procedure used by Elbashir et al. (2001). RNAi was assayed by flow cytometry after 24, 48, and 72 hours.

Transfection via electroporation

On the day before transfection, cells were split and cultured in RPMI supplemented with 10% FBS and IL-6. On the day of transfection, cells were spun down and washed once in Opti-MEM (Life Technologies Inc., Rockville, MD) before resuspension at a concentration of 20×10^6 cells or 400 μl. Cells were then incubated with 20 μg ErbB3-specific siRNA or the control fluorescein-labeled luciferase siRNA duplex for 10 minutes at ambient temperature in a 0.4-cm electroporation cuvette (BTX Genetronics, San Diego, CA). The cell/siRNA duplex mixture was pulsed once for 20 milliseconds at 250 V using a square wave electroporator (BTX Genetronics) and incubated at ambient temperature for 20 minutes prior to transferring cells to 6-well plates (Becton Dickinson) containing RPMI + 20% FBS + IL-6. RNAi was assayed by flow cytometry or Western blot analysis or both after 24, 48, 72, or 96 hours.

RESULTS AND DISCUSSION

We have had a longstanding interest in understanding the mechanisms underlying growth control of multiple myeloma cells. In this regard, we have employed a panel of disease-representative human myeloma cell lines that collectively display heterogeneity in cytokine responsiveness. Recent work in our laboratory focusing on receptor transactivation in this tumor model (French et al., 2002) led to the serendipitous discovery that ErbB3, a member of the epidermal growth factor receptor (EGFR) family, is atypically expressed in the multiple myeloma cell line, KAS-6/1 (D.K. Walters et al., unpublished observations). This finding was intriguing to us, as the KAS-6/1 cell line has also been shown to display an atypical growth response to interferon-α (IFN-α) (Westendorf et al., 1996). Consequently, we were interested in exploring the resulting phenotype of the KAS-6/1 cell line in the absence of ErbB3. Thus, the goal of the current study was to determine if RNAi could be used to induce gene silencing of ErbB3 in the myeloma cell line KAS-6/1.

As a first step, we designed an siRNA duplex that would specifically target ErbB3 using previously published guidelines for target design (Tuschl et al., 1999; Elbashir et al., 2001). Although siRNA duplexes have been shown to be effective at inducing RNAi in a number of adherent cell lines (Tuschl et al., 1999; Dudley et al., 2002; Tijsterman et al., 2002), successful use of this technology in nonadherent cells, for example, myeloma cells, had not been reported when we first began these studies. Therefore, before transfection of ErbB3 siRNA, it was first necessary to determine if the nonadherent KAS-6/1 cells could be transfected with dsRNA. To begin to address this question, we used several transfection protocols and tested our ability to transduce the KAS-6/1 cells with a preselected fluorescein-labeled duplex that targets the firefly luciferase plasmid (pGL2-Control) used by Elbashir et al. (2001). We chose this duplex because of our ability to assess transfection efficiencies by flow cytometry and because the KAS-6/1 cells do not express firefly luciferase and, therefore, should be unaffected by this dsRNA. We first employed Oligofectamine as a transfection reagent. We also used the same procedure described by Elbashir et al. (2001) that allowed these investigators to successfully transfect luciferase siRNA duplexes into a variety of luciferase-expressing adherent cell lines, including NIH/3T3, COS-7, HeLa S3, and 293 cells. In addition, we also evaluated the transfection ability of Cellfectin and DMRIE-C, a transfection reagent that is advertised as being specific for suspension cells. Fluorescence intensity was assessed by flow cytometry 24 hours after transfection. As seen in Figure 1A, an increase in fluorescence was detected in the KAS-6/1 cell line using all three transfection agents (Cellfectin, 59%; Oligofectamine, 66%; DMRIE-C, 77%). Of these three agents, however, DMRIE-C was clearly the most effective. As expected, no increase in fluorescence was observed when cells were incubated with siRNA in the absence of transfection agent. We concluded from these results that the fluorescein-labeled siRNA luciferase duplex could be successfully transfected into the KAS-6/1 cell line and that this transfection was most successful using DMRIE-C. Thus, DMRIE-C was used in subsequent experiments involving a transfection agent. Using all three reagents, we also assessed the effects of altering cell number or transfection agent concentration, and neither of these adjustments had a significant effect on transfection efficiency (data not shown).

The results demonstrated our ability to transduce labeled dsRNA into KAS-6/1 cells. We next wished to assess the ability of the ErbB3 siRNA duplex to silence

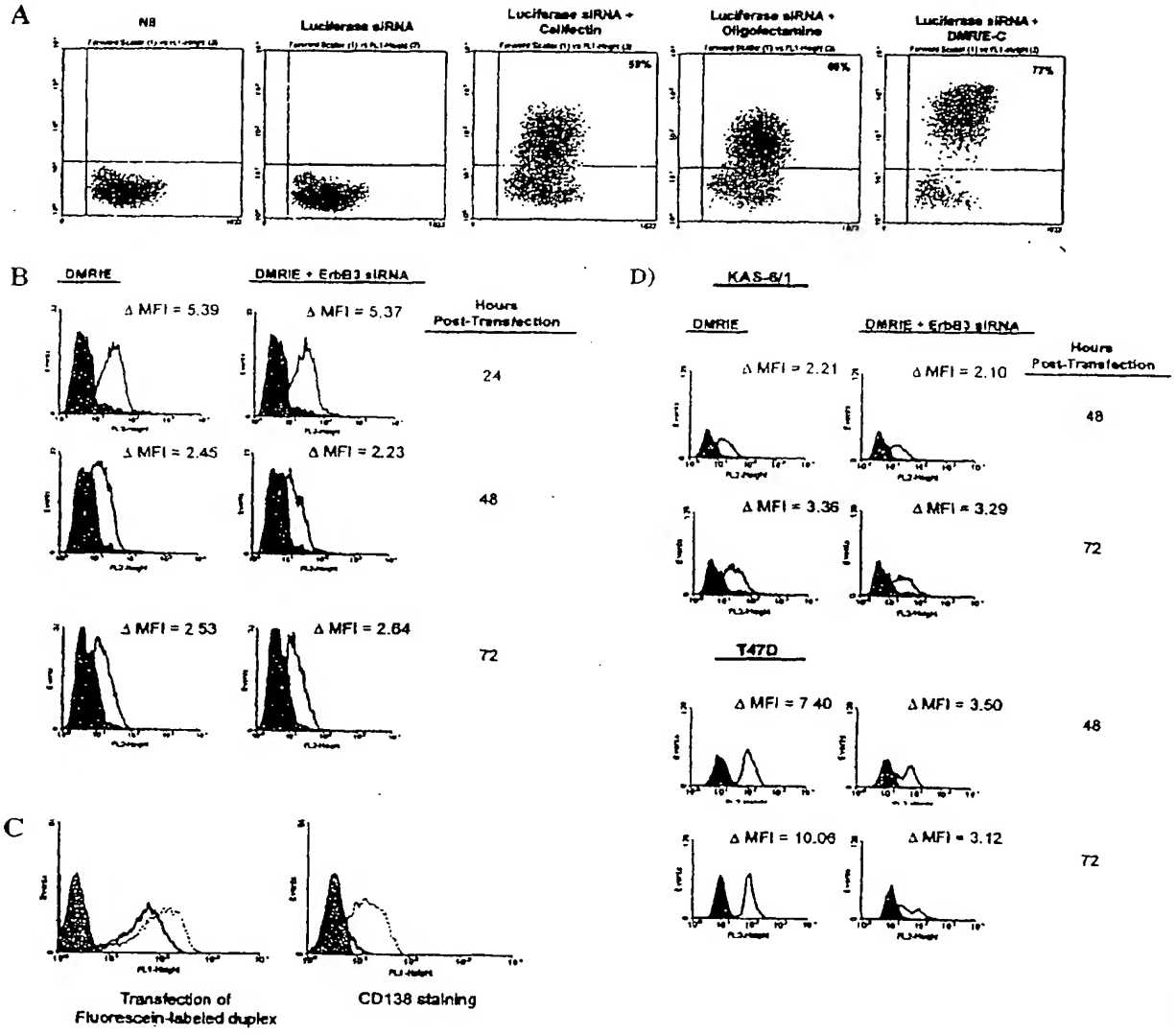

FIG. 1. Analysis of siRNA transfection efficiency and ErbB3 expression in myeloma cells following transfection with ErbB3 siRNA. (A) The KAS-6/1 myeloma cell line was transfected with fluorescein-labeled siRNA that targets the firefly luciferase plasmid. Fluorescence intensity was assessed by flow cytometry 24 hours after transfection. Nonspecific binding of siRNA to cells was assessed by incubating KAS-6/1 cells with siRNA in the absence of any transfection reagent (second panel from left). Forward scatter is shown on the X axis, and fluorescence intensity is shown on the Y axis. (B) KAS-6/1 cells were transfected with siRNA specifically targeting ErbB3 using DMRIE-C. Downregulation of ErbB3 surface expression was assessed 24, 48, and 72 hours after transfection using an ErbB3-specific mAb and flow cytometry. Isotype control, solid gray histogram; specific staining, solid line. (C) KAS-6/1 cells were transfected with fluorescein-labeled siRNA that targets the firefly luciferase plasmid. At 24 hours after transfection, cells were incubated with or without trypan blue before flow cytometric analysis. As a control, KAS-6/1 cells were incubated with an FITC-conjugated CD138 mAb and incubated with or without trypan blue prior to fixation. Isotype control, solid gray histogram; specific staining without trypan blue, dashed line; specific staining with trypan blue, solid line. (D) The KAS-6/1 myeloma cell line and the adherent T47D breast carcinoma cell line were transfected with siRNA specifically targeting ErbB3 using DMRIE-C. Downregulation of ErbB3 surface expression as assessed 48 and 72 hours after transfection via flow cytometry. Isotype control, solid gray histogram; specific staining, solid line.

ErbB3 expression, and we transfected the KAS-6/1 cells with the ErbB3 siRNA duplex using the protocol described and the DMRIE-C reagent. As a control, we also transfected cells with the fluorescein-labeled luciferase duplex. Overall transfection efficiency was assessed by FACS analysis of the percent positive fluorescent cells following transduction of the labeled duplex. Silencing of ErbB3 was assessed via flow cytometry. Similar to the previous experiments, an increase in fluorescence was detected following transfection of the fluorescein-labeled duplex (data not shown). However, when cells were transfected with the ErbB3-specific dsRNA complex, no significant decrease in surface expression of ErbB3 relative to mock-transfected cells could be detected (Fig. 1B). Thus, despite our ability to successfully transduce the labeled duplex, the ErbB3 siRNA duplex failed to alter ErbB3 expression. In additional experiments (results not shown), the ErbB3 siRNA duplex remained ineffective even after alteration of the duplex concentration, cell number, or transfection agent concentration.

Although the results shown in Figure 1A suggest that DMRIE-C was able to deliver dsRNA into the KAS-6/1

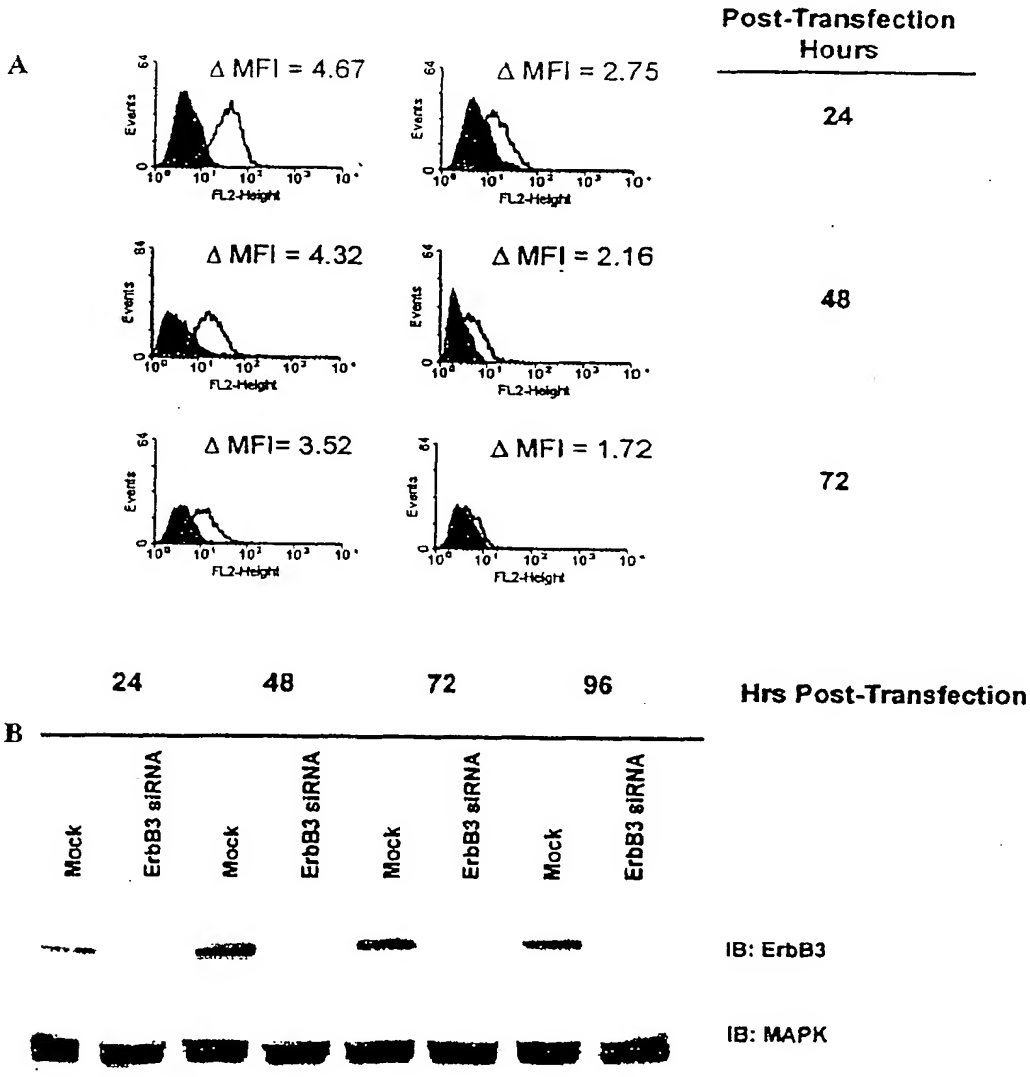

FIG. 2. Electroporation of KAS-6/1 cells with ErbB3-specific siRNA results in downregulation of ErbB3. (A) KAS-6/1 cells were transfected with ErbB3-specific siRNA via electroporation. Silencing of ErbB3 was assessed 24, 48, and 72 hours after transfection using an ErbB3 mAb and flow cytometry. Isotype control, solid gray histogram; specific staining, solid line. (B) Silencing of ErbB3 was also assessed by Western blot, following electrophoresis of whole cell lysates, using an ErbB3-specific Ab 24, 48, 72, and 96 hours after transfection.

cells, because the ErbB3-specific dsRNA complex was unable to modulate ErbB3 expression, it was possible that DMRIE-C simply facilitated cell surface binding of dsRNA but did not cause intracellular uptake. To address this possibility we again transfected the KAS-6/1 cells with the FITC-labeled duplex using DMRIE-C. Prior to fixation and flow cytometric analysis, we incubated the cells with or without trypan blue to assess extracellular vs. intracellular fluorescence. Of interest, although trypan blue was able to completely quench cell surface fluorescence as detected using an antibody to cell surface Syndecan-1 (Fig. 1C, right), trypan blue did not have a significant effect on the fluorescence signal emitted by KAS-6/1 cells transfected with the fluorescent dsRNA duplex (Fig. 1C, left). We conclude the majority of the duplex is successfully transfected into the KAS-6/1 cells using DMRIE-C and does not simply attach to the cell surface.

Although the manufacturer indicates that >70% of targets selected using the Tuschl et al. (1999) guidelines are successful in inducing RNAi of the respective gene of interest, it was possible that the ErbB3 siRNA duplex used in the studies described was simply an inefficient or ineffective ErbB3 target. To test this possibility, we trans-

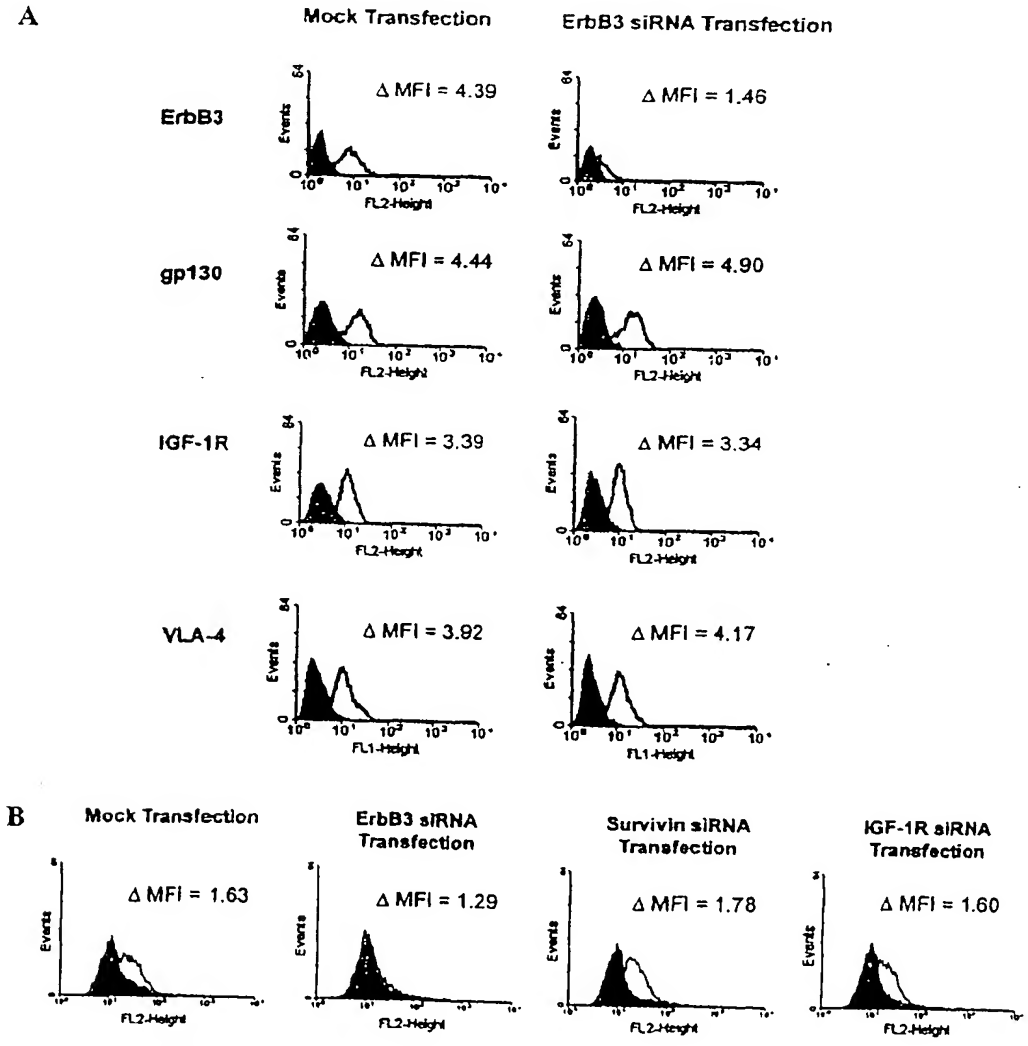

FIG. 3. Silencing of ErbB3 via RNAi is specific. (A) KAS-6/1 cells transfected with ErbB3 siRNA were assessed for expression of ErbB3, gp130, IGF-IR, and VLA-4 using receptor-specific Abs and flow cytometry 24 hours after transfection. (B) KAS-6/1 cells transfected with ErbB3 siRNA, survivin siRNA, or IGF-1R siRNA were assessed for downregulation of ErbB3 using an ErbB3-specific Ab and flow cytometry 24 hours after transfection.

fected T47D cells with the ErbB3 siRNA duplex using the transfection agent, DMRIE-C. T47D is an adherent breast carcinoma cell line that is known to express ErbB3. Gene silencing of ErbB3 was again assayed via flow cytometry using an ErbB3-specific antibody 48 and 72 hours after transfection. As shown in Figure 1C, transfection of the KAS-6/1 cell line with the ErbB3-specific siRNA duplex was again unsuccessful at silencing ErbB3 expression. However, significant downregulation of ErbB3 was observed in the T47D cells 48 and 72 hours after transfection. Thus, these data suggest that the ErbB3 siRNA target sequence is indeed functional at silencing ErbB3 and that its failure to silence ErbB3 in the KAS-6/1 cells must result from another factor(s).

To better understand why ErbB3-specific dsRNA duplex was ineffective in the KAS-6/1 cells, we again used the fluorescent duplex and used fluorescence microscopy to study intracellular localization after transfection. Of interest, we observed a cytoplasmic punctate staining pattern (results not shown). This pattern of localization to discrete foci is similar to the findings reported by Byrom et al. (2002) when they transfected fluorescently labeled c-*myc* siRNA into HeLa S3 cells. Similarly, when Coonrod et al. (1997) studied the efficiency of various DNA plasmid transfection methods, they reported that lipofection or Ca_2PO_4 transfection or both resulted in an initial granularlike accumulation of plasmid near the cell surface, with nuclear accumulation occurring over time. In contrast, it was reported that transfection via electroporation resulted initially in a more uniform staining of the cytoplasm. From these observations, Coonrod et al. concluded that the electroporation-induced pores most likely allowed more direct access to the soluble portion of the cytosol, whereas DNA transfected via lipofection may have to be sorted through endosomes and lysosomes before entering the cytoplasm or nucleus. It is possible, therefore, that although liposome-based transfection agents did permit siRNA duplex entry into the KAS-6/1 cell line, the accessibility of these duplexes to the RISC in these cells may be restricted.

To test this possibility, we next wished to determine if we could introduce the ErbB3 siRNA duplex into the KAS-6/1 cell line by electroporation. We have previously used electroporation to transduce expression plasmids into the KAS-6/1 cell line (French et al., 2002). We incubated the KAS-6/1 cell line with or without the ErbB3 siRNA duplex for 10 minutes and then electroporated the cells using 250 V for 20 milliseconds. There was striking downregulation of ErbB3, as revealed by flow cytometry and Western blot analysis, in the KAS-6/1 cell line as early as 24 hours after transfection (Fig. 2). Furthermore, this downregulation was maintained in the KAS-6/1 cell line over the 96-hour period. Alteration of voltage or siRNA duplex concentration did not have any significant effect on transfection efficiency or degree of silencing (data not shown). From these results, we concluded that the ErbB3 siRNA target is functional for silencing and that the RNAi pathway cannot be activated in the KAS-6/1 myeloma cell line with siRNA duplexes using cationic lipid or liposome-based transfection agents. However, transfection of siRNA duplexes targeting ErbB3 by electroporation was very efficient in inducing RNAi-mediated downregulation of ErbB3. Of particular interest, transfection of the T47D adherent breast carcinoma cell line with ErbB3 siRNA via electroporation caused a superior level of silencing of ErbB3 (data not shown) compared with the level of silencing achieved when using the transfection agent DMRIE-C. These data suggest that electroporation is an efficient method to induce RNAi in cells that appear to be resistant to siRNA transfection using commercial transfection agents. These data also suggest that electroporation may be an even more effective method of inducing RNAi in cells that are not resistant to transfection using commercial transfection agents. Wilda et al. (2002) were able to successfully transfect the nonadherent cell line K562 with siRNA using commercial carriers, suggesting that not all nonadherent cell lines will require transfection of siRNA via electroporation. However, our results raise the possibility that certain cell types may be uniquely sensitive to the mode of siRNA delivery and that electroporation may be a method to achieve more effective induction of siRNA, even in cell lines that are responsive to siRNA transfection using commercial carrier agents. The precise mechanisms underlying the success of the electroporation approach remain to be defined, but as alluded to, we speculate that this method is superior at facilitating access of the siRNA to the RNA-induced silencing complex.

Finally, we further assessed the specificity of RNAi-induced downregulation of ErbB3 by examining the expression levels of a variety of other surface molecules after treatment of the KAS-6/1 cells with the ErbB3 siRNA duplex. Figure 3A indicates that although ErbB3 expression was almost completely inhibited, surface levels of gp130, the IGF-1R, and VLA-4 were unaffected. To further test the specificity of RNAi in KAS-6/1 cells, we also treated these cells with dsRNA duplexes targeting survivin and the IGF-IR and compared the effects of these siRNA reagents with the ErbB3 siRNA on ErbB3 expression 24 hours after transfection. As can be seen in Figure 3B, downregulation of ErbB3 was observed only after transfection of ErbB3 siRNA, thus indicating the exquisite ability of this duplex to specifically silence ErbB3. Collectively, our results add to the literature demonstrating the feasibility of using RNAi in nonadherent cells and illustrate the importance of the method of cell transfection.

ACKNOWLEDGMENTS

This work was supported by National Institutes of Health grants CA62242 and CA62228.

REFERENCES

BYROM, M., PALLOTTA, V., BROWN, D., and FORD, L. (2002). Visualizing siRNA in mammalian cells: Fluorescence analysis of the RNAi effect. Ambion Technotes 9(3) (*www.ambion.com/techlib/tn/93/935.html*).

COONROD, A., LI, F.-Q., and HORWITZ, M. (1997). On the mechanism of DNA transfection: Efficient gene transfer without viruses. Gene Ther. 4, 1313–1321.

DUDLEY, N.R., LABBE, J.C., and GOLDSTEIN, B. (2002). Using RNA interference to identify genes required for RNA interference. Proc. Natl. Acad. Sci. USA 99, 4191–4196.

ELBASHIR, S.M., HARBORTH, J., LENDECKEL, W., YALCIN, A., WEBER, K., and TUSCHL, T. (2001). Duplexes of 21-nucleotide RNAs mediate RNA interference in cultured mammalian cells. Nature **411**, 484–498.

FIRE, A., XU, S., MONTGOMERY, M.K., KOSTAS, S.A., DRIVER, S.E., and MELLO, C.C. (1998). Potent and specific genetic interference by double-stranded RNA in *Caenorhabditis elegans*. Nature **391**, 806–811.

FRENCH, J.D., TSCHUMPER, R.C., and JELINEK, D.F. (2002). Analysis of IL-6-mediated growth control of myeloma cells using a gp130 chimeric receptor approach. Leukemia **16**, 1189–1196.

HAMMOND, S.M., CAUDY, A.A., and HANNON, G.J. (2001). Post-transcriptional gene silencing by double-stranded RNA. Nature Rev. Gen. **2**, 110–119.

HANNON, G.J. (2002). RNA interference. Nature **418**, 244–257.

HARBORTH, J., ELBASHIR, S.M., BECHERT, K., TUSCHL, T., and WEBER, K. (2001). Identification of essential genes in cultured mammalian cells using small interfering RNAs. J. Cell Sci. **114**, 4557–4565.

HUTVAGNER, G., and ZAMORE, P.D. (2002). RNAi: Nature abhors a double-strand. Curr. Opin. Genet. Dev. **12**, 225–232.

LI, L., MAO, J., SUN, L., LIU, W., and WU, D. (2002). Second cysteine-rich domain of Dickkopf-2 activates canonical Wnt signaling pathway via LRP-6 independently of Dishevelled. J. Biol. Chem. **277**, 5977–5981.

MATULIENE, J., and KURIYAMA, R. (2002). Kinesin-like protein CHO1 is required for the formation of midbody matrix and the completion of cytokinesis in mammalian cells. Mol. Biol. Cell **13**, 1832–1845.

TIJSTERMAN, M., KETTING, R.F., OKIHARA, K.L., SIJEN, T., and PLASTERK, R.H. (2002). RNA helicase MUT-14-dependent gene silencing triggered in *C. elegans* by short antisense RNAs. Science **295**, 694–697.

TUSCHL, T., ZAMORE, P.D., LEHMANN, R., BARTEL, D.P., and SHARP, P.A. (1999). Targeted mRNA degradation by double-stranded RNA *in vitro*. Genes Dev. **13**, 3191–3197.

VAN AMERSFOORT, E.S., and VAN STRIJP, J.A. (1994). Evaluation of a flow cytometric fluorescence quenching assay of phagocytosis of sensitized sheep erythrocytes by polymorphonuclear leukocytes. Cytometry **17**, 294–301.

WESTENDORF, J.J., AHMANN, G.J., GREIPP, P.R., WITZIG, T.E., LUST, J.A., and JELINEK, D.F. (1996). Establishment and characterization of three myeloma cell lines that demonstrate variable cytokine responses and abilities to produce autocrine interleukin-6. Leukemia **10**, 866–876.

WILDA, M., FUCHS, U., WOSSMANN, W., and BORKHARDT, A. (2002). Killing of leukemic cells with a BCR/ABL fusion gene by RNA interference (RNAi). Oncogene **21**, 5716–5724.

Address reprint requests to:
Dr. D.F. Jelinek
200 First Street, S.W.
Rochester, MN 55905

E-mail: jelinek.diane@mayo.edu

Received August 28, 2002; accepted in revised form October 18, 2002.

APPENDIX E

Short Technical Reports

Targeting the Kinesin Eg5 to Monitor siRNA Transfection in Mammalian Cells

BioTechniques 33:1244-1248 (December 2002)

ABSTRACT

RNA interference, the inhibition of gene expression by double-stranded RNA, provides a powerful tool for functional studies once the sequence of a gene is known. In most mammalian cells, only short molecules can be used because long ones induce the interferon pathway. With the identification of a proper target sequence, the penetration of the oligonucleotides constitutes the most serious limitation in the application of this technique. Here we show that a small interfering RNA (siRNA) targeting the mRNA of the kinesin Eg5 induces a rapid mitotic arrest and provides a convenient assay for the optimization of siRNA transfection. Thus, dose responses can be established for different transfection techniques, highlighting the great differences in response to transfection techniques of various cell types. We report that the calcium phosphate precipitation technique can be an efficient and cost-effective alternative to Oligofectamine™ in some adherent cells, while electroporation can be efficient for some cells growing in suspension such as hematopoietic cells and some adherent cells. Significantly, the optimal parameters for the electroporation of siRNA differ from those for plasmids, allowing the use of milder conditions that induce less cell toxicity. In summary, a single siRNA leading to an easily assayed phenotype can be used to monitor the transfection of siRNA into any type of proliferating cells of both human and murine origin.

INTRODUCTION

Post-transcriptional gene silencing by double-stranded RNA (RNA interference) is a widespread regulatory pathway among eukaryotes (17). Since its initial observation in *Caenorhabditis elegans*, two primary steps of the underlying mechanism have been identified. Long double-stranded molecules are first processed by an RNase III homolog, DICER, into short oligonucleotides [small interfering RNA (siRNA)] with a duplex region of approximately 19-nucleotide and 2-nucleotide 3′ overhangs (1,7). These siRNA are then incorporated into the RNA-induced silencing complex (RISC), creating a sequence-specific nuclease (8). In most vertebrate cells, the presence of double-stranded RNA induces the interferon response pathway, which includes the nonspecific inhibition of translation and RNA degradation (18). By contrast, short double-stranded oligonucleotides of the size generated by DICER are poor inducers, if at all, of the interferon response. Elbashir et al. (5) were the first to demonstrate the feasibility of using siRNA to inhibit gene expression in mammalian cells. Since then, additional reports have confirmed this observation with a growing set of genes, suggesting that this approach will be a major tool for functional genomics in mammalian cells (4,9).

In addition to being almost universal in terms of gene targeting, RNA interference can probably be implemented in a wide variety of cellular contexts. Indeed, although it is still possible that some differentiated cells lack the interfering machinery, there is at this point no documented example of this in mammals. Currently, there appears to be two main aspects to optimize when implementing RNA interference. First, since the RISC recognizes its target through sequence complementarity, it can be expected that the accessibility of the corresponding sequence plays a important role in the efficiency of silencing. Accordingly, the efficiency of silencing can differ significantly between oligoribonucleotides that target different sequences along the same mRNA (10). The second limitation is the penetration of siRNA into cells. Although a direct uptake of oligonucleotides takes place in *Drosophila* S2 cells, a transfection procedure is usually required in mammalian cells. Elbashir and coworkers (5) have reported that for cell lines commonly used for plasmid transfections (e.g., HeLa and NIH 3T3), Oligofectamine™ (Invitrogen SARL, Cergy Pontoise, France) could be used to introduce siRNA in up to 90% of the cells. However, this protocol cannot be simply transposed to all cell types. Thus, the first difficulty with implementing RNA interference in a new cell type is optimizing the transfection procedure. In particular, it is well known that it is difficult to introduce nucleic acids in hematopoietic cells. In this report we show that an oligonucleotide that targets the Eg5 mRNA provides a powerful tool for optimizing transfection protocols for siRNA.

MATERIALS AND METHODS

Cell Culture

HeLa cells and F9 subclone were routinely maintained in DMEM supplemented with 10% FCS. For monoastrol treatment, the cells were incubated for 16 h in 100 µM monoastrol (Tocris, Fisher Bioblock Scientific, Illkirch, France).

The K562 cell line was originally established from the pleural effusion of a patient with chronic myeloid leukemia (12), and the UT7 cell line was established from a patient with megakaryoblastic leukemia (11). These cell lines were maintained in α-MEM (Invitrogen SARL) supplemented with 10% FCS and 5 ng/mL recombinant human granulocyte/macrophage-colony stimulating factor (generously provided by Novartis Pharma S.A., Rueil Malmaison, France).

Transfection Procedure

Eg5 oligoribonucleotides were purchased as purified and protected reagents from MWG-Biotech (Courtaboeuf, France). The sequence of the Eg5 sense and antisense strands were 5′-CUGAAGACCUGAAGACAAUdTdT-3′ and 5′-AUUGUCUUCAGGUCUUCAGdTdT-3′, respectively (centered on position 2263 of GenBank® accession number NM_004523). The sequence of the mutated Eg5 sense and antisense strands were 5′-CACCUCAUAUUCCUUAUCGdTdT-3′ and 5′-CGAUAAGGAAUAUGAGGUGdTdT-3′ (centered on position 1065 of GenBank accession number NM_004523; note

that this nucleotide, which is normally a G, is replaced by an A in this mutated sequence). Oligonucleotides were deprotected as recommended by the manufacturer and resuspended in water. Sense and antisense strands were hybridized as previously described (5). The same oligoribonucleotides purchased from other sources, such as Dharmacon (Boulder, CO, USA) and Genset (Paris, France), had similar efficiencies. Moreover, unpurified oligonucleotides were as active as purified ones, while being shipped in larger amounts.

Transfection using Oligofectamine was performed as recommended by the manufacturer. Briefly, 10^5 cells were seeded in 3.5 cm dishes 16 h before transfection. Transfection was performed using 3 µL Oligofectamine reagent per dish and the indicated amount of siRNA or antisense RNA.

Transfection by calcium phosphate precipitation was performed by a standard procedure (15). Briefly, 10^5 cells were seeded in 3.5 cm dishes 24 h before transfection. The siRNA was diluted with 1 mM Tris, pH 7.8, 0.1 mM EDTA to a final volume of 36.8 µL. We then added 5.2 µL 2.5 M $CaCl_2$ and 42 µL 2× HBS (50 mM HEPES, 280 mM NaCl, 10 mM KCl, and 1.5 mM Na_2HPO_4, adjusted to pH 7.05 with NaOH), and precipitation was triggered by air bubbling through the solution (injecting twice with the pipetman a volume of air corresponding to its last setting, which is 42 µL). After 20 min, 84 µL precipitate were added to one dish. Following an overnight incubation at 37°C, the culture medium was renewed. For RNA preparation, the protocol was scaled up for 10-cm dishes with 5×10^5 cells and 500 µL precipitate. The silencing efficiency was reproducible and independent from the scale of the experiment.

For electroporation, K562 or UT7 cells were washed twice with serum-free IMDM and resuspended to a final concentration of 10^7 cells/mL in opti-MEM™ (Invitrogen SARL). Subsequently, 0.2 mL cell suspension were mixed with different concentrations of siRNA and electroporated with a Bio-Rad® apparatus. Three different conditions were tested: 300 V and 125 µF; 280 V and 250 µF; and 260 V and 960 µF. The cell viability following electroporation was assessed by 7-aminoactinomycin D staining. The 280 V/250 µF condition was the most efficient for silencing and was used for the dose-response analysis.

Immunofluorescence

Cells were grown and transfected on glass coverslips or, alternaltively, treated with monoastrol, and the resulting floating cells were spun on a glass coverslip using a cytospin. Cells were then fixed by incubation in methanol for 3 min at -20°C. After rehydration in PBS, the cells were incubated with rabbit anti-Eg5 polyclonal antibody or mouse anti-β tubulin monoclonal 2.1 antibody (Sigma-Aldrich, Lyon, France), and then with a Texas Red-coupled goat anti-rabbit or Rho-coupled goat anti-mouse IgG $F(ab)_2$ fragment (Jackson ImmunoResearch Laboratories, West Grove, PA, USA). The DNA was stained with 4′,6 diamino-2-phenylindole (DAPI), 0.25 µg/mL (Sigma-Aldrich). Coverslips were mounted in Citifluor mounting media (Citifluor Ltd, London, UK). Imaging of immunofluorescence was performed by confocal laser scanning on a Leica TCS-NT/SP (Leica, Heidelberg, Germany), equipped with an air-cooled Argon-Krypton mixed-gas laser and an APOCHROMAT 63× 1.32 oil immersion objective.

Western Blot Analysis

Twenty micrograms of protein were separated on a 6.5% SDS-polyacrylamide gel and transferred on a nitrocellulose BAS83 membrane (Schleicher & Schuell, Ecquevilly, France). The membrane was incubated with rabbit anti-Eg5 or anti-Kif15 polyclonal antibodies and then with peroxidase-coupled goat anti-rabbit IgG (Jackson ImmunoResearch Laboratories) and revealed with the SuperSignal® West Pico Chemiluminescent Signal kit (Perbio Science, Bezons, France).

Cell Cycle Analysis

The cells were washed in PBS containing 0.5% paraformaldehyde and 0.5% saponin (Sigma Chemical, France) at 4°C for 5 min and then incubated in PBS containing 5 µg/mL propidium iodide (Sigma-Aldrich) and 100 µg/mL RNase A at 4°C for 2 h. The samples were then analyzed with a FACSort™ (BD Biosciences, San Jose, CA, USA), and the percentage of cells in the G2/M phase of the cell cycle was calculated using the MultiCycle software (Phoenix Flow Systems, San Diego, CA, USA).

RESULTS AND DISCUSSION

Eg5 is a kinesin-related motor that is involved in the assembly of the mitotic spindle and the migration of chromosomes along the mitotic spindle (16). Inhibition of Eg5 activity, either by microinjection of antibodies (2) or with a specific drug such as monoastrol (14), leads to a monopolar spindle and an arrest of cells in prometaphase. Therefore, inducing a degradation of Eg5 mRNA by RNA interference was expected to lead to a similar phenotype. In this study we used a 19-nucleotide-long duplex RNA with 2-nucleotide 3′ overhangs that corresponded to a sequence of the Eg5 coding region that is conserved between man and mouse. In HeLa cells, the introduction of this siRNA with Oligofectamine induced an accumulation of cells in prometaphase and the appearance of monopolar spindles (Figure 1A). This phenotype was only observed with double-stranded oligonucleotides and was comparable with that observed in the presence of monoastrol (Figure 1A). A similar result was reported by Elbashir and co-workers (6,9) with another oligonucleotide targeting the Eg5 mRNA. To confirm that the arrest in prometaphase was due to Eg5 mRNA degradation, Eg5 RNA and protein levels were analyzed on cells transfected 48 h earlier with increasing doses of siRNA. Semiquantitative RT-PCR analysis of Eg5 mRNA revealed a decrease at the lowest dose analyzed, 30 ng per 3-cm dish, reaching 70% at 3 µg per dish. In parallel experiments, Western blots indicated a 60% decrease in protein levels at the 3-µg dose. From these bulk analyses, it is not possible to assess precisely the level of suppression with no knowledge of the percentage of cells that have received the oligonucleotide. Together, these results support the in-

duction of a specific degradation of Eg5 mRNA, leading to an arrest in prometaphase.

While RNA and protein assays are technically demanding and require specific tools, a blockage in prometaphase can be detected through a variety of experimental approaches, some of which are easily accessible. For adherent cells, the loss of adhesion to the substrate provides the simplest indication of a blockage in prometaphase. Figure 1B illustrates with HeLa cells how this phenotype can be observed by routine inspection under phase contrast microscopy. Moreover, the phenotype was already detectable 24 h after transfection, indicating a rapid blockage of the cell cycle. Because of this rapid re-

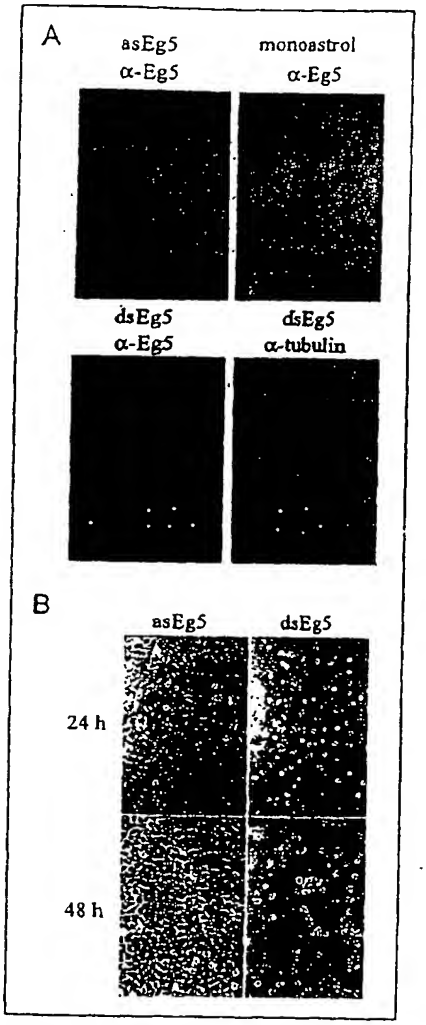

Figure 1. Eg5 siRNA transfection in HeLa cells. (A) Phenotypic analysis of HeLa cells treated with monoastrol, Eg5 antisense RNA (asEg5), or siRNA (dsEg5). Cells were transfected with Oligofectamine or treated with 100 µM monoastrol for 16 h. Twenty-four hours after transfection or following monoastrol treatment, Eg5, tubulin, and DNA were detected using indicated antibodies (red) and DAPI (blue), respectively. Fluorescence was analyzed by confocal microscopy at 630× magnification. (B) Phase contrast microscopy of transfected HeLa cells. The culture was analyzed by phase contrast microscopy at 100× magnification 24 h and 48 h after transfection with either antisense (asEg5) or si RNA (dsEg5).

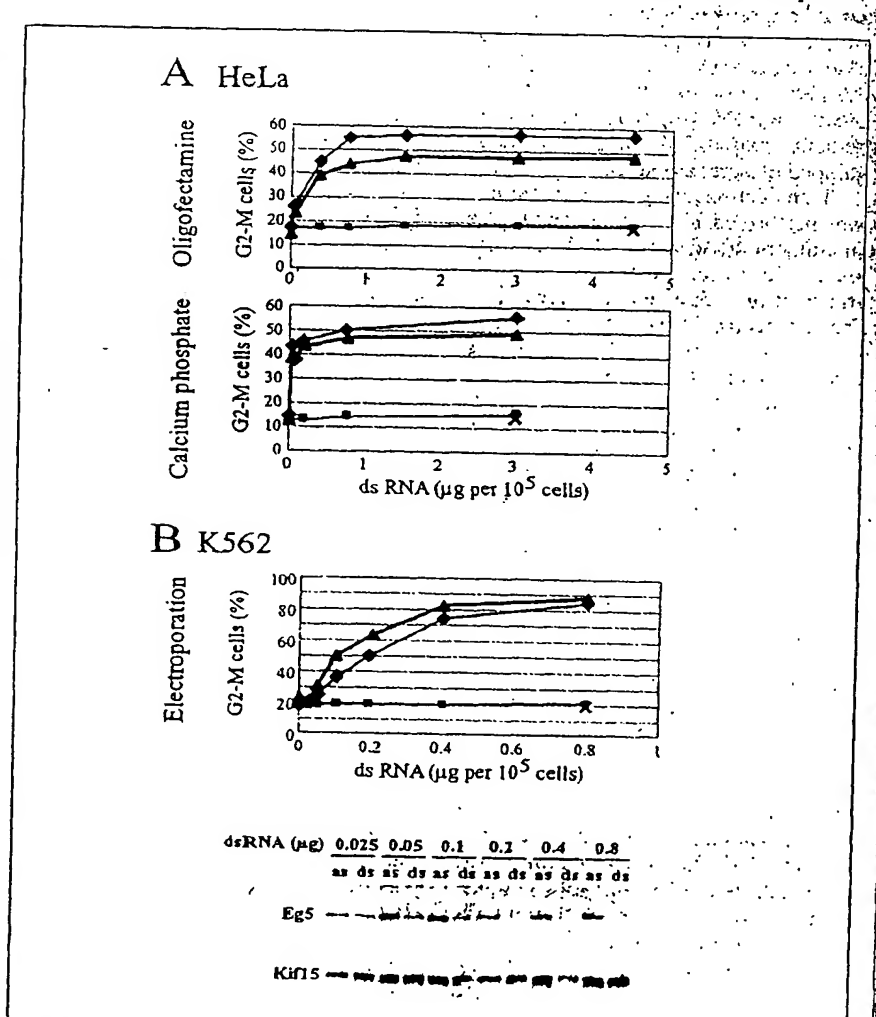

Figure 2. Dose-response analysis of mitotic arrest following Eg5 dsRNA transfection. (A) Dose response in HeLa cells. Cells were transfected with the indicated dose of Eg5 duplex (solid symbols) or antisense RNA (gray squares) using Oligofectamine (upper panel) or calcium phosphate precipitation (lower panel). Two independent experiments are presented with the Eg5 duplex, one with the antisense oligonucleotide. For comparison, the result observed with a mutated Eg5 duplex diverging from the human sequence by one nucleotide is indicated by a cross. The analysis of the cell cycle 48 h after transfection was performed by cytofluorometry after DNA staining with propidium iodide. The percentage of cells in the G2/M phase of the cell cycle was plotted as a function of the RNA dose. (B) Dose response in K-562 cells. K562 cells were transfected with the indicated dose of Eg5 duplex (solid symbols) or antisense RNA (gray squares) by electroporation at 280 V and 250 µF. Two independent experiments are presented with the Eg5 duplex, one with the antisense oligonucleotide, and the result observed with a mutated duplex is indicated by a cross. Cell cycle analysis was performed as in panel A and is presented on the upper panel. An aliquot of the cells transfected by the antisense (as) or duplex (ds) RNA was used to extract the proteins, and Eg5 expression was analyzed by Western blot analysis along with a Kif15 control (lower panel).

sponse, the activity of Eg5 siRNA can also be measured by simply counting the cells 24 h or 48 h after transfection.

Precise quantification of the growth arrest phenotype induced by Eg5 siRNA can be achieved through cytofluorometry. Figure 2A illustrates the use of this approach to measure a dose response of HeLa cells to two different transfection techniques: Oligofectamine and calcium phosphate precipitation. Cytofluorometry was performed on cells stained with propidium iodide 48 h after transfection. Because both transfection protocols entail the creation of inhomogeneous solutions, the doses are expressed in micrograms per 10^5 cells rather than in concentration. Using Eg5 double-stranded oligonucleotides, similar plateaus were reached with both procedures, where 50% to 60% of the cells accumulating in G2/M. For each technique, very reproducible dose responses were observed in independent experiments. Although it has recently been reported that an antisense oligonucleotide could induce gene silencing under some circumstances, the antisense Eg5 oligonucleotide did not exhibit any significant activity in our experiments (13). In addition, a double-stranded oligonucleotide diverging from the human sequence by one nucleotide did not show any activity at the highest dose, which confirms the specificity of the observed phenotype. Importantly, with the calcium phosphate transfection, the plateau was reached with a significantly lower amount of siRNA (100 ng/10^5 cells). Calcium phosphate precipitation is a low-cost transfection procedure that can be performed on large scales that are well adapted to biochemical studies. Our results establish the suitability and the cost effectiveness of this strategy for RNA interference studies. In addition, these results indicate that the penetration of siRNA is more efficient than that of plasmids, as such high transfection efficiency cannot be achieved for these longer molecules even in transient assays.

For cells growing in suspension, calcium phosphate precipitation is inappropriate, while liposomes and cationic lipids give unpredictable results on a new cell line. Electroporation can, a priori, be adapted to all cell types, although high-transfection efficiencies are usually associated with a high cellular toxicity. Reasoning that, similar to calcium phosphate, the requirements for the penetration of siRNA are likely to be different from those of plasmids, we expected that less harsh electroporation conditions could lead to an efficient penetration of siRNA. To explore this possibility, we first used the erythroleukemic cell line K 562, for which efficient conditions of electroporation of long nucleic acid molecules have been reported (19). Using the Eg5 siRNA, we tested electroporation conditions with respect to the arrest in prometaphase and the viability of cells. At 280 V and 250 µF, the viability of cells following electroporation was higher than 85%. Figure 2B presents a dose response to the Eg5 siRNA. At 0.8 µg per 10^5 cells, from 85% to 90% of the cells accumulated in G2/M (Figure

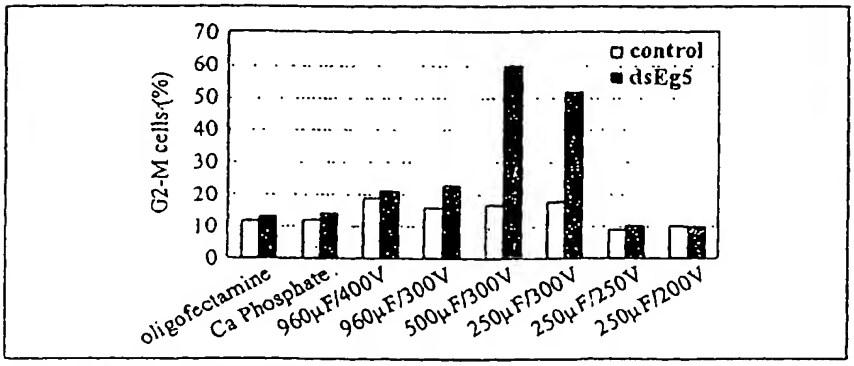

Figure 3. Test experiment on a HY subclone. The HY subclone was mock transfected (control) or transfected with the Eg5 duplex RNA using the indicated transfection procedure. Cell cycle analysis was performed as in Figure 2A, 36 h after transfection.

2B, upper panel). These results indicate that electroporation can enable the penetration of siRNA in a vast majority of the cells. A parallel analysis by Western blot confirmed an important decrease in Eg5 protein (Figure 2B, lower panel). Moreover, the residual expression at the different doses of siRNA correlated with the percentage of cells unaffected in their cell cycle and that presumably had not been transfected. Similar results in terms of both the efficiency of cell cycle arrest and cell viability were obtained with the megakaryocytic cell line UT7 in spite of the low efficiency of plasmid transfection commonly observed in this cell line (data not shown).

Several aspects of Eg5 biology make it an excellent indicator for monitoring RNA interference. First, the endogenous Eg5 gene is expressed in all the proliferating cells that have been analyzed to date. Second, its activity is required for mitosis, and therefore the penetration of siRNA systematically results in an inhibition of growth. This growth inhibition can be evaluated by several approaches that are accessible to all laboratories, from cell counting to DAPI staining and either microscopy or cytofluorometry. Finally, the action of Eg5 siRNA is rapid and best analyzed between 30 h and 48 h. The evaluation of siRNA transfection in a new cell type can therefore be easily monitored with no specific reagents required, provided the targeted cells are proliferating. To illustrate the practical value of Eg5 siRNA, Figure 3 summarizes the testing of different transfection protocols in a subclone of the F9 murine teratocarcinoma cell line. Neither Oligofectamine nor calcium phosphate induced a significant accumulation of cells in G2/M, indicating a low efficiency of transfection. We then explored the feasibility of using electroporation. By varying the parameters of the electrical impulse, conditions could be found that led to an accumulation in G2/M comparable to that observed in HeLa cells (Figure 2A). This result confirmed that, as expected, the same siRNA can be used in murine and human cells. Again, these parameters led to a low cellular toxicity, confirming that the penetration of siRNA does not require transfection protocols as drastic as those for plasmids.

Recently, expression vectors have been designed to enable the synthesis of appropriate siRNA precursors within cells (3). While this can result in a long-term inhibition of the target gene, this strategy entails the transfection of standard plasmids with all the associated limitations. Besides, the use of in vitro synthesized siRNA provides a great flexibility in testing target sequences and for large-scale screenings. Our results illustrate that an efficient transfection of siRNA can be achieved in various cell types, and the Eg5 siRNA provides a versatile tool for the choice and the optimization of the transfection protocol.

REFERENCES

1. **Bernstein, E., A.A. Caudy, S.M. Hammond, and G.J. Hannon.** 2001. Role for a bidentate ribonuclease in the initiation step of RNA interference. Nature *409*:363-366.
2. **Blangy, A., H.A. Lane, P. d'Herin, M. Harper, M. Kress, and E.A. Nigg.** 1995. Phosphorylation by p34cdc2 regulates spindle association of human Eg5, a kinesin-related motor essential for bipolar spindle formation in vivo. Cell *83*:1159-1169.
3. **Brummelkamp, T.R., R. Bernards, and R. Agami.** 2002. A system for stable expression of short interfering RNAs in mammalian cells. Science *296*:550-553.
4. **Caplen, N.J., S. Parrish, F. Imani, A. Fire, and R.A. Morgan.** 2001. Specific inhibition of gene expression by small double-stranded RNAs in invertebrate and vertebrate systems. Proc. Natl. Acad. Sci. USA *98*:9742-9747.
5. **Elbashir, S.M., J. Harborth, W. Lendeckel, A. Yalcin, K. Weber, and T. Tuschl.** 2001. Duplexes of 21-nucleotide RNAs mediate RNA interference in cultured mammalian cells. Nature *411*:494-498.
6. **Elbashir, S.M., J. Harborth, K. Weber, and T. Tuschl.** 2002. Analysis of gene function in somatic mammalian cells using small interfering RNAs. Methods *26*:199-213.
7. **Elbashir, S.M., W. Lendeckel, and T. Tuschl.** 2001. RNA interference is mediated by 21- and 22-nucleotide RNAs. Genes Dev. *15*:188-200.
8. **Hammond, S.M., E. Bernstein, D. Beach, and G.J. Hannon.** 2000. An RNA-directed nuclease mediates post-transcriptional gene silencing in Drosophila cells. Nature *404*:293-296.
9. **Harborth, J., S.M. Elbashir, K. Bechert, T. Tuschl, and K. Weber.** 2001. Identification of essential genes in cultured mammalian cells using small interfering RNAs. J. Cell Sci. *114*:4557-4565.
10. **Holen, T., M. Amarzguioui, M.T. Wiiger, E. Babaie, and H. Prydz.** 2002. Positional effects of short interfering RNAs targeting the human coagulation trigger tissue factor. Nucleic Acids Res *30*:1757-1766.
11. **Komatsu, N., H. Nakauchi, A. Miwa, T. Ishihara, M. Eguchi, M. Moroi, M. Okada, Y. Sato, et al.** 1991. Establishment and characterization of a human leukemic cell line with megakaryocytic features: dependency on granulocyte-macrophage colony-stimulating factor, interleukin 3, or erythropoietin for growth and survival. Cancer Res. *51*:341-348.
12. **Lozzio, C.B. and B.B. Lozzio.** 1975. Human chronic myelogenous leukemia cell-line with positive Philadelphia chromosome. Blood *45*:321-334.
13. **Martinez, J., A. Patkianowska, H. Urlaub, R. Lührmann, and T. Tuschl.** 2002. Single-stranded antisense siRNAs guide target RNA cleavage in RNAi. Cell *110*:563-574.
14. **Mayer, T.U., T.M. Kapoor, S.J. Haggarty, R.W. King, S.L. Schreiber, and T.J. Mitchison.** 1999. Small molecule inhibitor of mitotic spindle bipolarity identified in a phenotype-based screen. Science *286*:971-974.
15. **Sambrook, J., E.F. Fristsch, and T. Maniatis.** 1989. Molecular Cloning. CSH Laboratory Press, Cold Spring Harbor, NY.
16. **Sawin, K.E., K. LeGuellec, M. Philippe, and T.J. Mitchison.** 1992. Mitotic spindle organization by a plus-end-directed microtubule motor. Nature *359*:540-543.
17. **Sharp, P.A.** 2001. RNA interference—2001. Genes Dev. *15*:485-490.
18. **Stark, G.R., I.M. Kerr, B.R. Williams, R.H. Silverman, and R.D. Schreiber.** 1998. How cells respond to interferons. Annu. Rev. Biochem. *67*:227-264.
19. **Van Tendeloo, V.F., P. Ponsaerts, F. Lardon, G. Nijs, M. Lenjou, C. Van Broeckhoven, D.R. Van Bockstaele, and Z.N. Berneman.** 2001. Highly efficient gene delivery by mRNA electroporation in human hematopoietic cells: superiority to lipofection and passive pulsing of mRNA and to electroporation of plasmid cDNA for tumor antigen loading of dendritic cells. Blood *98*:49-56.

We are grateful to A. Vervisch for technical help with flow cytometry. This work was supported by the Centre National de la Recherche Scientifique. *Address correspondence to Dr. Michel Kress, CNRS UPR1983, Institut André Lwoff, 7 rue Guy Môquet, 94801 Villejuif cedex, France. email: kress@infobiogen.fr*

Received 9 July 2002; accepted 8 October 2002.

D. Weil, L. Garçon[1], M. Harper, D. Duménil[1], F. Dautry, and M. Kress
CNRS UPR1983
Institut André Lwoff
[1]INSERM U362
Institut Gustave Roussy
Villejuif, France

APPENDIX F

Am J Physiol Endocrinol Metab 292: E884–E890, 2007.
First published November 22, 2006; doi:10.1152/ajpendo.00569.2006.

Reduction of *O*-GlcNAc protein modification does not prevent insulin resistance in 3T3-L1 adipocytes

Katherine A. Robinson, Lauren E. Ball, and Maria G. Buse
Department of Medicine, Division of Endocrinology, Diabetes, and Medical Genetics, Medical University of South Carolina, Charleston, South Carolina

Submitted 20 October 2006; accepted in final form 16 November 2006

Robinson KA, Ball LE, Buse MG. Reduction of *O*-GlcNAc protein modification does not prevent insulin resistance in 3T3-L1 adipocytes. *Am J Physiol Endocrinol Metab* 292: E884–E890, 2007. First published November 22, 2006; doi:10.1152/ajpendo.00569.2006.—3T3-L1 adipocytes develop insulin-resistant glucose transport upon preincubation with high (25 mM) glucose, provided that insulin (0.6 nM) is included, Akt activation is impaired, and high glucose and insulin act synergistically. Considerable evidence suggests that increased glucose flux via the hexosamine biosynthesis pathway enhances the *O*-GlcNAc modification (*O*-GlcNAcylation) of some critical protein(s) that may contribute to insulin resistance. However, whether enhanced protein *O*-GlcNAcylation is necessary for the development of insulin resistance is unknown. We used two strategies to test this hypothesis. The first strategy was the overexpression of *O*-GlcNAcase, which removes *O*-GlcNAc from Ser/Thr of proteins. Cells were infected with *O*-GlcNAcase-expressing adenovirus (or empty virus) 5 days before they were submitted to protocols that elicit (or not) insulin resistance. *O*-GlcNAcase was highly expressed and functional as assessed by Western blot, *O*-GlcNAcase assay, and marked reduction of *O*-GlcNAcylated proteins. The activity was mainly cytosolic. The second strategy was the expression of *O*-GlcNAc transferase (OGT) being markedly reduced by transfection of OGT siRNA, resulting in an approximately 90% decrease of nuclear and cytosolic OGT protein expression and similar reduction in *O*-GlcNAcylated proteins. Nontargeting siRNA had no effect. Preincubation in high glucose with low-dose insulin decreased the acute insulin response of glucose transport by at least 50% and impaired Akt activation. None of these parameters were affected by overexpression of *O*-GlcNAcase or by OGT knockout. Excess *O*-GlcNAcylation is one of many factors that can cause insulin resistance. It does not seem to be required for the development of glucose/insulin-induced insulin resistance of glucose transport and Akt activation in 3T3-L1 adipocytes.

glucose transport; Akt activation; *O*-linked *N*-acetylglucosamine

INSULIN RESISTANCE IS A HALLMARK of type 2 diabetes and is associated with uncontrolled type 1 diabetes, obesity, and the metabolic syndrome, as well as numerous other conditions such as cystic fibrosis, polycystic ovary syndrome, uremia, septicemia, glucocorticoid excess, and others. Clinically, insulin resistance is defined as the decreased ability to lower plasma glucose in response to a given dose of insulin. By this definition, it would reflect primarily impaired insulin-stimulated glucose transport into cells that express the glucose transporter GLUT4 (skeletal muscle, heart muscle, and adipocytes).

Sustained hyperglycemia causes insulin resistance in humans (34) and in animal models (27), which leads to the concept of glucose toxicity. It accounts for the insulin resistance observed in patients with uncontrolled type 1 diabetes, which is reversible with insulin therapy (34). Similarly, sustained elevations of circulating nonesterified fatty acids also cause insulin resistance (lipotoxicity). Thus insulin resistance may be the cells' answer to the provision of excess nutrients. Several investigators (1, 20, 28) have proposed that increased flux through the hexosamine synthesis pathway (HSP) may function as a cellular nutrient sensor and play a role in the development of insulin resistance and the complications of diabetes. The role of HSP in the development of insulin resistance was first proposed by Marshall et al. (19) in 1991 and was based on studies in isolated rat adipocytes. Ever since then, a relatively copious literature that has recently been reviewed (2) has developed on this subject.

The HSP is a minor branch of the glycolytic pathway; glucose entry into HSP is catalyzed by the first and rate-limiting enzyme glutamine:fructose-6-phosphate (F-6-*P*) amidotransferase (GFAT), which converts F-6-*P* and glutamine into glucosamine 6-phosphate (GlcN-6-*P*) and glutamate. GlcN-6-*P* is metabolized to UDP-*N*-acetylglucosamine (UDP-GlcNAc), the major product of the pathway (19). UDP-GlcNAc and other amino sugars generated by the pathway provide building blocks of glycosyl side chains for proteins and lipids. UDP-GlcNAc is also the obligatory substrate of *O*-linked *N*-acetylglucosamine (*O*-GlcNAc) transferase (OGT), a cytosolic and nuclear enzyme that modifies Ser/Thr residues of certain proteins by attaching single GlcNAc moieties in *O*-linkage (17, 18). *O*-GlcNAcylation frequently occurs on transcription factors and often involves known phosphorylation sites, suggesting a regulatory role (3). The process is reversible; *O*-GlcNAc is removed by a specific enzyme, *O*-GlcNAcase (32).

The synergistic effects of preincubation in high glucose and insulin on the development of insulin-resistant glucose transport in primary adipocytes were first reported by Garvey et al. (10). This model has been widely used to study the mechanisms of glucose-induced insulin resistance. We (23–25) have characterized it in some detail in 3T3-L1 adipocytes. Briefly, preincubation (18 h) in high (25 mM) glucose causes down-regulation of subsequent, acutely insulin-stimulated glucose transport, provided that low-dose (0.6 nM) insulin is included during preincubation. Preincubation in low (5 mM) glucose with insulin, or with high glucose without insulin, does not mimic the effect. The expression of glucose transporters (GLUT4 and GLUT1) is unaffected, and so is the proximal

Address for reprint requests and other correspondence: M. G. Buse, 96 Jonathan Lucas St., CSB 823, Charleston, SC 29425 (e-mail: busemg@musc.edu).

The costs of publication of this article were defrayed in part by the payment of page charges. The article must therefore be hereby marked "*advertisement*" in accordance with 18 U.S.C. Section 1734 solely to indicate this fact.

insulin-signaling cascade, as judged by inulin receptor substrate-1-associated phosphatidylinositol 3-kinase activity (23). However, both chronic exposure to low-dose insulin and high glucose independently impair acute insulin activation of Akt, and the two effects are synergistic (25). Since the effects of excess glucose flux via the HSP could be mediated by excess *O*-GlcNAc modification of some signaling protein(s) (21, 30, 31), we felt that overexpression of *O*-GlcNAcase in 3T3-L1 adipocytes, before they are submitted to conditions that promote insulin resistance, or inhibition of OGT by RNA interference (RNAi) would serve to test this hypothesis.

MATERIALS AND METHODS

Adenovirus preparation. pcDNA3.1His *O*-GlcNAcase (a generous gift from Dr. G. W. Hart) was digested with *NotI*/*XbaI* and ligated into pAdTrack.CMV (19, 20). Plasmids were prepared using Plasmid Mini and Maxi Kits (Qiagen). Homologous recombination with pAdEasy-1 was performed in *Escherichia coli* BJ5183 cells (Stratagene). Recombinants were selected and transformed into *E. coli* XL-1 Blue (Stratagene), and large-scale plasmid preparations were generated as above. An empty vector preparation without the *O*-GlcNAcase insert was prepared in parallel. The adenovirus coexpresses green fluorescent protein (GFP). Adenovirus generation and amplification were performed in human embryonic kidney 293 cells as described (13, 14) and were purified using BD Adeno-X virus purification kit (BD BioSciences). Adenovirus concentration was determined by limiting dilution plaque assay and by spectrophotometric measurement.

To assess whether facilitated targeting of *O*-GlcNAcase into the nucleus affects insulin sensitivity, an *O*-GlcNAcase cDNA construct was prepared with a COOH-terminal nuclear targeting sequence and a c-myc tag for the generation of recombinant adenovirus. Human *O*-GlcNAcase was cut out of the pAdTrack vector with *NotI* and *Hin*dII. The pShooter pCMV/nuc/myc vector (Invitrogen) containing three repeats of the nuclear localization signal (DPKKKRKV) and a c-myc tag (EQKLISEEDL) was linearized with *NotI* and filled in prior to cutting with *XbaI*. The *O*-GlcNAcase and the nuclear targeting sequence/c-myc tag were then ligated into the *NotI*/*XbaI* sites of pBluescriptSK-. Using site-directed mutagenesis (Quickchange; Stratagene) and the following primer, the stop codon between *O*-GlcNAcase and the nuclear targeting sequence was replaced with alanine, 5′-GGTCGGAGCCTGGCGGCCTTGTTGGCCGC-3′. The insert was then cut out of pBluescript SK- with *NotI*/*XbaI*/*Ssp*I, and the 2,694-bp fragment was ligated into the *NotI*/*XbaI* sites of the pAdTrack vector. The *O*-GlcNAcase/nuc/myc pAdTrack vector was linearized with *Pme*I and electroporated into BJ5183-AD-1 electrocompetent cells (Stratagene), following the protocol supplied by the manufacturer. Production of the virus was performed as described above, following the protocol of He et al. (13).

Viral infection of 3T3-L1 adipocytes and glucose transport assay. 3T3-L1 fibroblasts were differentiated into adipocytes as described (23). On *day 6* of the differentiation protocol they were infected with 2×10^8 pfu/ml (MOI 200) empty or *O*-GlcNAcase adenovirus in serum-free DMEM for 4 h at 37°C followed by addition of FCS (to 10%) and incubation overnight. Fresh growth medium was applied. Five days after infection (~90% of cells expressing GFP), cells were incubated for 18 h in DMEM 1% FCS medium containing either 5 mM glucose or 25 mM glucose plus low-dose insulin (6×10^{-11} to 6×10^{-10} M). Cells were serum and insulin deprived for 2 h and then stimulated or not for 15 min with either a low dose of insulin, which resulted in half-maximal stimulation of glucose transport (6×10^{-11} M), or with a fully stimulating insulin dose (4×10^{-10} to 10^{-7} M), and glucose transport measured as the uptake of 2-deoxyglucose for 3 min, as previously described (23).

Total postnuclear extracts of cells were prepared in lysis buffer (50 mM HEPES, pH 7.4, 140 mM NaCl, 1 mM EDTA, 1 mM NaF, 1 mM sodium pyrophosphate, 100 μM sodium vanadate, 1% Triton X-100, and 10 μg/ml leupeptin, aprotinin, and pepstatin A, 1 mM phenylmethanesulfonyl fluoride, and 1 μM microcystin LR). Glucose transport was quantified by scintillation counting of a portion of the extract. Protein determination using Coomassie Protein Reagent (Pierce), *O*-GlcNAcase enzyme assays, and Western blots were also performed using these extracts. Nuclear extracts were prepared using the method of Dignam et al. (7).

RNAi. To reduce OGT expression, a small interfering RNA (siRNA) to a sequence in the COOH-terminal region of mouse OGT (Ref. NM-139144.2) corresponding to nucleotides 3420–3440 was transfected. This sequence was chosen on the basis of recent successful OGT suppression by an siRNA targeted against this region of rat OGT (11) that differs from the mouse in one nucleotide. The sequence of the siRNA against mouse OGT was sense 5′AGGGAACUAGAUAACAUGCUU-3′. For the control, scrambled siRNA, the sequence was sense 5′-CGCAUUAAUCUAGUUCGCUUU-3′. A BLAST search of GenBank was carried out to avoid matches with other known sequences. Custom siRNA synthesis was carried out by Dharmacon (Lafayette, CO). This siRNA resulted in 50–60% suppression of OGT protein expression in 3T3-L1 adipocytes. To obtain a more complete suppression of OGT expression, we purchased SMARTpool Reagent from Dharmacon, which consists of a mixture of 4 unique siRNAs developed against the targeted gene and is guaranteed to silence the RNA by ≥75%. Transfection of this preparation decreased OGT protein expression by ~90% in 3T3-L1 adipocytes. For cells treated with nontargeting siRNA, we used Dharmacon's non-targeting siRNA pool of 4.

siRNA transfection or electroporation. 3T3-L1 adipocytes are difficult to transfect, and until recently, successful siRNA transfection was achieved only via electroporation (22). Recently, a technology using virus-derived amphipatic peptides has been developed (6) that directly interacts with nucleic acid cargos to form nanoparticles that diffuse through plasma membranes and release their cargos inside the cell. The technology has been adapted by the manufacturer (Genospectra, Fremont, CA) to several cell lines that are difficult to transfect, including 3T3-L1 adipocytes. We adopted the following protocol for transfection of the latter.

On *day 6* after initiation of the differentiation protocol, cells were subcultured to a density of 2.5×10^4 cells/cm^2 and incubated overnight in DMEM containing 25 mM glucose and 10% FCS. Then, FCS was removed and cells were washed with PBS and transfected with a final concentration of 40 nM nontargeting or OGT siRNA using the Express-si Delivery Kit (Genospectra). Following a 4-h incubation with the siRNA, FCS was added to a concentration of 10%, and cells were incubated for an additional 18 h. Medium was replaced with fresh DMEM containing 25 mM glucose and 10% FCS for 24 h. Cells were then incubated for 18 h in DMEM containing 1% FCS and 5 mM glucose or 25 mM glucose plus 0.6 nM insulin and then serum and insulin deprived for 2 h and glucose transport measured as described.

For electroporation, on *day 6* after initiation of the differentiation protocol, 7×10^6 cells were trypsinized, washed, and resuspended in PBS and electroporated with 20 nmol of scrambled or OGT siRNA, using the Gene Pulser XCell (Biorad) at a setting of 975 μF, 180 V, exponential decay in a 0.4-mm gap cuvette. Following electroporation, DMEM containing 25 mM glucose and 10% FCS was added to the cells, and they were plated at a density of 1.75×10^6 cells/cm^2. Medium was refreshed the following day. Forty-eight hours after electroporation, cells were incubated in DMEM containing 1% FCS and 5 mM glucose or 25 mM glucose plus 0.6 nM insulin for 18 h and then serum and insulin deprived for 2 h and glucose transport measured as described.

Western blots of phosphorylated Akt, O-GlcNAcase, OGT, and O-GlcNAc-modified proteins. Cell extracts (20 μg protein) were separated on 7% SDS-PAGE and transferred to nitrocellulose. For

Western blot of phosphorylated (p)-Akt, *O*-GlcNAcase, and OGT, membranes were blocked for 1 h and then incubated overnight in 50 mM Tris, pH 7.4, 150 mM NaCl, 0.05% Tween 20, 5% nonfat dry milk (blocking buffer) containing anti-p-Akt rabbit polyclonal antibody (1:1,000, Cell Signaling), or anti-*O*-GlcNAcase or anti-OGT rabbit polyclonal antibody (1:5,000 and 1:2,000 respectively, both gifts of Dr. G. W. Hart). Following washing, membranes were incubated in goat anti-rabbit IgG (1:10,000, Jackson Immunoresearch) for 1 h, washed, developed with West Pico ECL Reagent (Pierce), exposed to film, and quantified by photodensitometry using a National Institutes of Health Image Analyzer.

For detection of *O*-GlcNAc-modified proteins, membranes were processed using the *O*-GlcNAc Western blot detection kit (Pierce), which uses the 110.6 antibody, developed by Comer et al. (4). In some experiments an alternative anti-*O*-GlcNAc antibody (RL-2, which was originally discovered as recognizing nuclear pore proteins), obtained from Affinity Bioreagents, was used.

O-GlcNAcase assay (modified from Refs. 8 and 9). Cell extracts (100 μl) were incubated for 30 min at 37°C in a final volume of 200 μl containing 50 mM sodium cacodylate, pH 6.4, 0.3% BSA, 2 mM *p*-nitrophenyl *N*-acetyl-β-D-glucosaminide (*p*-NPAGA), and 50 mM *N*-acetylgalactosamine without or with an *O*-GlcNAcase inhibitor, *O*-(2-acetamido-2-deoxy-D-glucopyranosylidene)-amino-*N*-phenylcarbamate [PUGNAC (1 μM); Toronto Research Chemicals], which served as background. Reactions were stopped by the addition of 1.8 ml of 50 mM sodium carbonate, and A_{400} was determined (ϵ^{mM} = 17.7). *O*-GlcNAcase activity was determined by subtracting the +PUGNAC blank and expressed as micromoles of *p*-NPAGA per milligram extract protein per minute.

Materials. Unless otherwise indicated in the text, materials were purchased from Sigma.

RESULTS

3T3-L1 adipocytes were infected with the *O*-GlcNAcase adenovirus or with empty virus on *day 6* of the differentiation protocol, as described in MATERIALS AND METHODS. The time of infection was chosen because cells were easier to infect before they were fully differentiated. At the time of the experiment (5 days postinfection), >95% of the cells expressed the full adipocyte phenotype and >90% expressed GFP, indicating viral infection. On inspection under the microscope there were no obvious morphological differences between cells infected with empty or *O*-GlcNAcase-expressing adenovirus or noninfected cells.

To assess the level of expression of *O*-GlcNAcase, the enzyme activity was measured in postnuclear supernatants. The enzyme activity was increased >10-fold in cell extracts prepared from cells infected with *O*-GlcNAcase virus compared with cells expressing the empty virus. The conditions of preincubation of the cells (low or high glucose) made no difference (Fig. 1*A*). Figure 1*B* shows Western blots of postnuclear supernatants prepared from cells, as shown in Fig. 3, and developed with an antibody that specifically recognizes *O*-GlcNAc-modified proteins [antibody 110.6 (Ref. 4)]. Cells that were infected with empty virus and preincubated in high glucose showed clearly increased *O*-GlcNac modification of numerous proteins (Fig. 1*B*, *lane 3*), and this was diminished in cells overexpressing the *O*-GlcNAcase virus (Fig. 1*B*, *lane 4*). Figure 1*C* again demonstrates the enzyme activity in cell extracts using another antibody, RL-2. In comparing cells preincubated in high glucose expressing empty or *O*-GlcNAcase adenovirus, the latter showed a marked reduction in *O*-GlcNAc-modified proteins. Cells that were infected with adenovirus expressing *O*-GlcNAcase showed a strongly reactive band on Western blot developed with *O*-GlcNAcase antibody; the antibody was not sensitive enough to detect endogenous *O*-GlcNAcase in total cell extracts of cells infected with empty virus (Fig. 1*D*). Taken together, the data indicate that

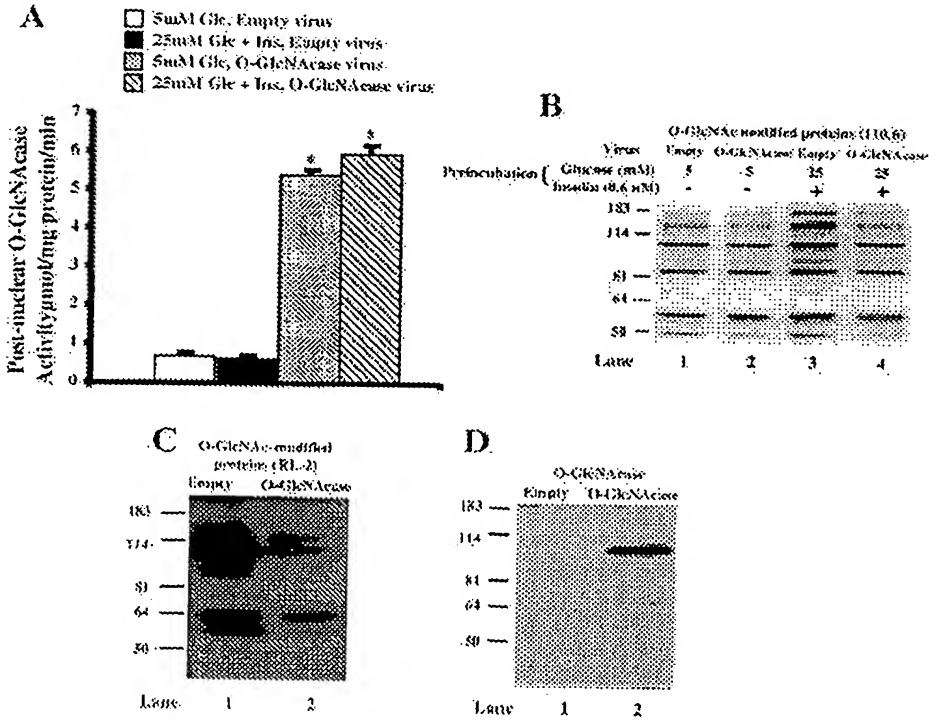

Fig. 1. *O*-GlcNAcase amount and activity are markedly increased in cells infected with *O*-GlcNAcase virus. *A*: *O*-GlcNAcase activity was measured in postnuclear supernatants of cell lysates infected with the adenovirus expressing the enzyme or cells infected with empty virus using a method modified from Gao et al. (9), as described in MATERIALS AND METHODS. Means + SE are shown; n = 16 observations from 4 separate experiments. *B*: Western blots prepared from postnuclear supernatants of cell lysates developed with an antibody (110.6, Pierce) that specifically recognizes *O*-GlcNAc-modified proteins. 3T3-L1 adipocytes, which had been incubated for 18 h with 25 mM glucose plus 0.6 nM insulin, show clearly increased *O*-GlcNAcylation of several protein bands if infected with empty virus. However, total *O*-linked *N*-acetylglucosamine (*O*-GlcNAc) modification is diminished in cells overexpressing OGlcNAcase. *C*: the same cells developed with another *O*-GlcNAc-specific antibody, RL-2 (Affinity Bioreagents). *O*-GlcNAcylation is reduced in cells overexpressing *O*-GlcNAcase. *D*: Western blot developed with an anti-*O*-GlcNAcase antibody of postnuclear supernatants prepared from cells preincubated in high glucose plus 0.6 nM insulin and infected with empty virus (*lane 1*) or with *O*-GlcNAcase virus (*lane 2*).

the cells infected with adenovirus strongly expressed O-GlcNAcase and that the enzyme was functional.

Cells were incubated for 18 h in DMEM containing 1% FBS and either 5 mM glucose or 25 mM glucose plus low-dose insulin (6×10^{-11} to 6×10^{-10}M). Cells were then deprived of FCS and insulin for 2 h, stimulated or not (basal) for 15 min with a half-maximally or maximally stimulating dose of insulin, before measuring glucose transport for 3 min. As shown in Fig. 2, pretreating cells with high glucose plus insulin downregulated subsequent basal and insulin-stimulated glucose transport in response to both half-maximal and maximal insulin stimulation by ~40% ($P < 0.03$-$P < 0.001$). Insulin stimulation above basal (Δinsulin) was also significantly reduced at both acute insulin concentrations. However, there was no significant difference in downregulation between cells infected with O-GlcNAcase virus or the empty virus.

Since preincubation in high glucose plus low-dose insulin downregulates Akt activation by acute insulin (25), we next tested this parameter. Cells were preincubated in 5 mM glucose or in 25 mM glucose plus 6×10^{-10} M insulin, deprived of serum and insulin for 2 h, and then stimulated with 10^{-7} M insulin for 15 min. Figure 3 illustrates a Western blot developed with an antiphosphoserine Akt (p-Akt) antibody. In the basal state, the p-Akt signal was too weak for graphic illustration. After acute stimulation by insulin, there was a robust p-Akt signal that was approximately twice as strong in cells preincubated in low glucose as it was in cells exposed to high glucose plus insulin. However, overexpression of O-GlcNAcase did not protect the cells from downregulation, and there was no significant difference in the level of p-Akt between cells infected with empty virus and O-GlcNAcase virus.

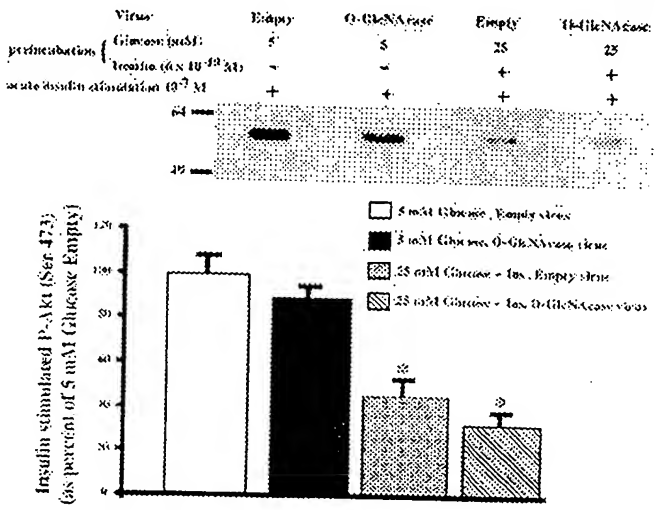

Fig. 3. O-GlcNAcase overexpression fails to restore the impaired activation of Akt by acute insulin stimulation in cells preincubated in high glucose plus low-dose insulin. Cells were treated as described in Fig. 1. Postnuclear supernatants were prepared from detergent-treated cell lysates in the presence of phosphatase and protease inhibitors. Proteins were separated by SDS-PAGE and immunoblotted with a p-Akt antibody that recognizes $pSer^{473}$. *A*: representative Western blot. Basal Akt phosphorylation was too low to quantify. The bands shown are from cells that were acutely stimulated with insulin (10^{-7} M). *B*: results from 4 experiments. Data are normalized to Akt phosphorylation after acute insulin stimulation in cells preincubated in 5 mM glucose and infected with empty virus. Means + SE are shown; $n = 4$. *Significantly different from corresponding cells preincubated in 5 mM glucose. The expression of O-GlcNAcase had no significant effect.

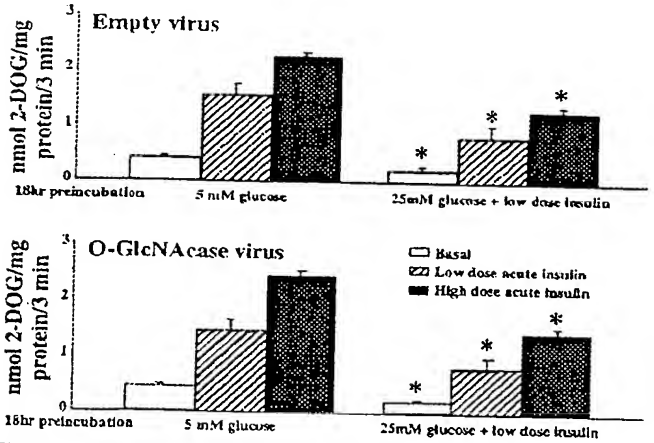

Fig. 2. Overexpression of O-GlcNAcase does not affect the development of insulin resistance in cells preexposed to high glucose plus low-dose insulin. 3T3-L1 adipocytes were infected with adenovirus expressing O-GlcNacase or with empty virus 5 days before experiments. More than 90% of cells expressed adenovirus, and 95% were fully differentiated at the time of the experiment. Cells were preincubated for 18 h with either 5 mM glucose or 25 mM glucose plus low-dose insulin (6×10^{-11} to 6×10^{-10} M), serum and insulin deprived for 2 h, and then either not stimulated (basal) or stimulated for 15 min with insulin at a half-maximally or maximally stimulating dose. Glucose transport was then measured for 3 min [as 2-deoxyglucose (2-DOG) transport]. Means + SE are shown; $n = 4$–8. *Significantly decreased from corresponding observation in cells pretreated with 5 mM glucose, $P < 0.02$–0.001. There are no differences between cells treated with O-GlcNAcase or empty virus.

Since the development of insulin resistance most likely involves transcriptional regulation, it was important to determine the site of expression of the O-GlcNAcase enzyme. As shown in Fig. 4*A*, the overexpressed O-GlcNAcase was restricted to the cytosol, where its activity was markedly increased in cells infected with the O-GlcNAcase-containing virus. However, the activity in the nucleus was much lower than in the cytosol and was similar in cells infected with empty virus or with virus expressing O-GlcNAcase, suggesting that the overexpressed enzyme penetrates the nucleus poorly. This finding was further confirmed by examining Western blots (Fig. 4*B*) prepared from nuclear extracts or cytosol of cells treated under the different conditions and developed with an antibody (110.6) that specifically recognizes O-GlcNAc-modified proteins (4). In the cytosol and in the nucleus there was a trend toward increased O-GlcNAc modification of proteins in cells infected with empty virus and exposed to 25 mM glucose and low-dose insulin. Although cells expressing O-GlcNAcase tended to demonstrate less O-GlcNAcylation in the nucleus (compare *lanes 2* and *4* in Fig. 4*B*), only in the cytosol was there a clear decrease in O-GlcNAc-modified proteins in cells overexpressing O-GlcNAcase after preincubation in low or in high glucose. (compare *lane 6* with *8* and *lane 5* with *7*). The fact that transfected O-GlcNAcase is mainly restricted to the cytosol has previously been noted in COS-7 cells (9).

Our attempt at increasing nuclear targeting of O-GlcNAcase by expressing it with a nuclear localization signal was not successful. Although active enzyme was expressed in the cytosol, its nuclear expression did not improve. It also failed to

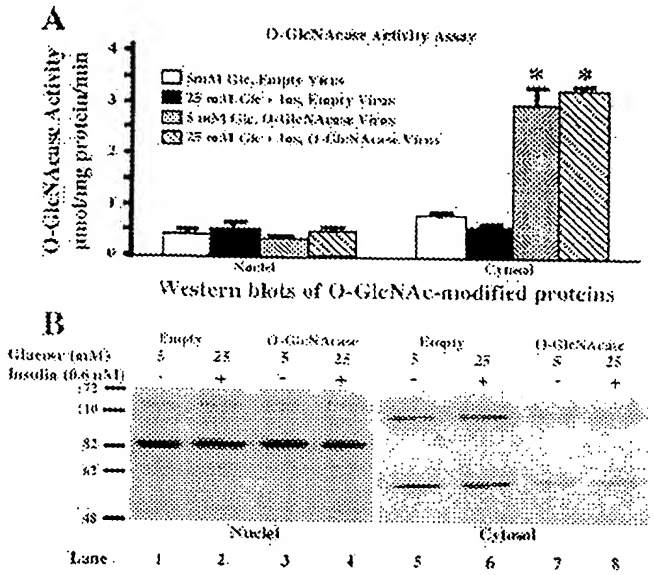

Fig. 4. Nuclear extracts show little evidence of increased *O*-GlcNAcase activity in cells infected with virus expressing the enzyme. Nuclear extracts were prepared as described in MATERIALS AND METHODS. The infranatant below the lipid layer overlying the nuclear pellet was designated cytosol. *A*: *O*-GlcNAcase activity measurements (as in Fig. 1*A*) in nuclear extracts and cytosol. Although the cytosol shows marked increases in *O*-GlcNAcase activity in cells infected with virus expressing the enzyme, there is no evidence of this in the nuclear extracts; $n = 3$ experiments. *Different from cells expressing empty virus, $P < 0.01$–0.001. *B*: Western blots of nuclear extracts or cytosol developed with an antibody (110.6 from Pierce) that specifically recognizes *O*-GlcNAc modified proteins. O-G, *O*-GlcNAcase-expressing virus. In cells infected with empty virus, there is a trend supporting increased glycosylation of proteins in cells preexposed to high glucose plus insulin. Although in the cytosol there is a marked decline in protein glycosylation in cells infected with *O*-GlcNAc-expressing virus, this trend is barely discernible in the nucleus (compare *lanes 2* and *4*). The gel is representative of 3 similar experiments.

have any effect on preventing the downregulation of the insulin response of glucose transport in cells preincubated in high glucose plus low-dose insulin (data not shown).

To rule out the possibility that the lack of effect of overexpressing *O*-GlcNAcase on the development of insulin resistance was due to some peculiarity of our adenoviral construct, we obtained an *O*-GlcNAcase-expressing adenovirus from Dr. W. H. Dillmann. Dr. Dillmann's group had successfully used this adenovirus to prevent the downregulation of sarcoplasmic reticulum Ca^{2+}-ATPase (SERCA2a) expression in cardiac myocytes incubated in high (25 mM) glucose (16). Results with this construct were essentially identical to those obtained with our *O*-GlcNAcase adenovirus. Although the activity was clearly overexpressed, it did not prevent the development of insulin resistance (data not shown).

Transfection or electroporation of OGT siRNA (developed to the COOH terminus) into 3T3-L1 adipocytes reduced the expression of OGT protein by 50–60% in 72 h, as assessed by Western blots. When the two methods were optimized, the results were very similar. However, overexpression of OGT siRNA again did not prevent the development of insulin resistance in cells preincubated in high glucose plus low-dose insulin. Preexposure to high glucose increased the *O*-GlcNAc modification of proteins, as assessed by 110.6 antibody staining, and this was decreased in cells transfected with OGT siRNA. The reduction of OGT expression was observed both in the cytosol and in nuclei, and results were similar upon introduction of siRNA by electroporation or by transfection (data not shown). Since these results may simply reflect that OGT was not sufficiently suppressed to mitigate the development of insulin resistance, we tested the SMARTpool Reagent (Dharmacon) consisting of a mixture of 4 siRNAs that are guaranteed to silence the desired RNA by ≥75%. In our case, OGT protein expression was decreased by ~90%, both in the cytosol and in nuclear extracts of 3T3-L1 adipocytes (Fig. 5*A*). Furthermore, the *O*-GlcNAc modification of proteins was markedly reduced both in the nuclei and in the cytosol of cells that had been treated with OGT siRNA (Fig. 5*B*). However, this did not affect either the basal or the insulin-stimulated glucose transport in cells preexposed to 5 mM glucose or to 25 mM glucose plus low-dose insulin and did not prevent or mitigate the development of insulin resistance in the latter (Fig. 5*C*). OGT knockdown also failed to restore the impaired insulin-stimulated Akt activation in insulin-resistant cells (Fig. 5*D*).

DISCUSSION

There is considerable evidence in the literature indicating that increased flux through the HSP, and specifically increased protein *O*-GlcNAcylation, can cause insulin resistance in adipocytes and in skeletal muscle (reviewed in Ref. 2). Mice overexpressing OGT in skeletal muscle and fat develop insulin resistance, as assessed by significantly reduced glucose disposal during hyperinsulinemic-euglycemic insulin clamp studies, as well as hyperleptinemia (21). Mice overexpressing the rate-limiting enzyme of the HSP, GFAT, in muscle and fat also develop insulin resistance (5, 15), which was evident in vivo (5, 15) but not in isolated muscle preparations and was attributed to cross talk between fat tissue and muscle (12). Obici (26) did not find evidence for insulin resistance, based on the hyperinsulinemic clamp technique, in mice overexpressing GFAT in skeletal muscle. Many authors base their conclusions on a link between insulin resistance and increased flux through the HSP on the observation that increased UDP-GlcNAc and insulin resistance tend to coexist, and the former enhances the rate of *O*-GlcNAc modification of proteins (2). Our observations do not negate the fact that increased protein *O*-GlcNAcylation can cause or contribute to insulin resistance of glucose transport and Akt activation; the experiments were designed to answer the question whether or not this process is required for its development.

There is strong evidence for a role of increased protein *O*-GlcNAc modification in the development of some of the complications of diabetes. In two cases, the techniques used here reversed the phenomenon; e.g., Dillmann reported that diabetic hearts showed increased protein *O*-GlcNAcylation as well as functional changes indicative of diabetic cardiomyopathy, such as contractile dysfunction and decreased expression of SERCA2a. All of these changes were reversed by treatment with *O*-GlcNAcase-expressing adenovirus (the adenovirus developed by Dillmann used the same plasmid construct as ours; both were gifts from G. W. Hart) (16). Similarly, exposure to high glucose induces plasminogen activator inhibitor-1 (PAI-1) expression in mesangial cells; this is mediated by enhanced

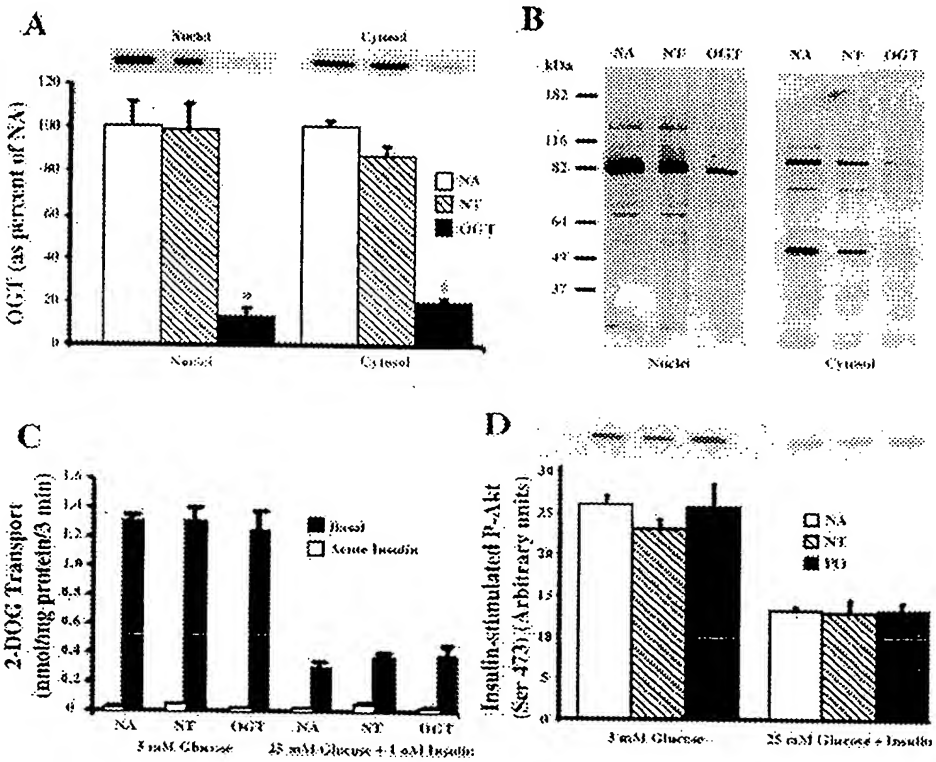

Fig. 5. Knockdown of *O*-GlcNAc transferase (OGT) does not prevent glucose/insulin-induced insulin resistance. In the experiments shown here, OGT knockdown was carried out using the "Smartpool Reagent"(Dharmacon), which consists of 4 unique siRNAs against mouse OGT; as nontargeting controls, we used Dharmacon's nontargeting siRNA pool of 4. Cells were transfected using a transfection reagent obtained from Genospectra, as described in MATERIALS AND METHODS, 48 h prior to initiating experiments and then cells were placed into conditions for 18 h, which will (or will not) cause insulin resistance. Thus cells were processed ~72 h after transfection. *A*: expression of OGT protein assessed by Western blots in nuclei and cytosol of cells that were incubated for 18 h in 25 mM glucose plus 0.6 nM insulin. NA, no RNA addition, although the cells underwent all the manipulations of the transfection protocol; NT, transfected with nontargeting siRNA; OGT, transfected with siRNA against OGT. *Top* of the graph shows a representative Western blot, whereas the bar graph (*bottom*) illustrates means + SE of 4 observations. *OGT < NA or NT, $P < 0.001$. *B*: representative Western blot of nuclear extracts and cytosol developed with the anti-*O*-GlcNAc antibody. The cells were transfected and preincubated under exactly the same conditions as in *A*, and the gel is representative of 4 similar experiments. Clearly, OGT knockdown markedly reduced protein *O*-GlcNAcylation both in the nucleus and in the cytosol. *C*: comparison of basal and maximally insulin-stimulated (0.1 uM) glucose transport between cells preincubated in 5 mM glucose, with cells preincubated in 25 mM glucose plus 0.6 nM insulin. High glucose/insulin caused insulin resistance, $P < 0.01$ vs. corresponding 5 mM glucose-treated cells. OGT knockdown had no effect; $n = 4$. *D*: same experimental design as *C*, except that insulin-stimulated Akt activation is studied, which is measured as the phosphorylation of Akt on Ser^{473}. Basal phosphorylation of Akt in this system is barely detectable and is not shown. Cells preincubated in high glucose plus low insulin demonstrated impaired insulin-stimulated Akt activation, $P < 0.01$. OGT knockdown had no effect; $n = 4$.

O-GlcNAcylation and transcriptional activation of Sp1. Inhibition of *O*-GlcNAcylation by enhanced *O*-GlcNAcase expression via adenovirus, or by decreasing the expression of OGT via siRNA, inhibited high glucose-mediated PAI-1 induction, thus clearly demonstrating a causal connection between *O*-GlcNAcylation and specific transcriptional events (11). The complete lack of response to the marked diminution of *O*-GlcNAc protein modification in our studies may suggest that the insulin resistance of our model cannot be modified. This, however, is not the case. We have found that the insulin resistance of glucose transport and Akt activation is partially reversed by brief treatment with rapamycin or with an inhibitor of classical protein kinase C (unpublished observations).

The limited nuclear penetration of overexpressed *O*-GlcNAcase had been previously noted by Gao et al. (9) in Cos-7 cells. Since the development of insulin resistance most likely involves transcriptional events, we initially thought that the lack of effect of *O*-GlcNAcase treatment may reflect the insufficient nuclear expression of the overexpressed enzyme. However, the experiments with OGT knockdown, where the enzyme was similarly decreased by ~90% in the nucleus and the cytosol, without affecting the development of insulin resistance, do not support this hypothesis. However, the limited nuclear transport of overexpressed *O*-GlcNAcase is of interest. Recent studies (29) have established that *O*-GlcNAcase is a bifunctional enzyme with activatable histone acetyl transferase and *O*-GlcNAcase activities. Furthermore, the enzyme associates strongly with OGT and accompanies it with histone deacetylases into transcription corepression complexes (33). These characteristics may be unfavorable for nuclear transport, at least in some cells. In cardiac myocytes (16) and in glomerular mesangial cells (11), *O*-GlcNacase penetrated the nucleus sufficiently to affect transcription.

In conclusion, overexpression of OGT in muscle and fat causes insulin resistance in vivo (21). However, the fact that two maneuvers that markedly reduced *O*-GlcNAcylation, in-

cluding reducing OGT expression by ~90%, failed to prevent or mitigate glucose/insulin-induced insulin resistance suggests that excess *O*-GlcNAcylation is only one of many causative factors of insulin resistance. Increased *O*-GlcNAcylation does not seem to be required for the development of insulin resistance of glucose transport and Akt activation in this model in 3T3-L1 adipocytes.

ACKNOWLEDGMENTS

We gratefully acknowledge the gift of antibodies to *O*-GlcNAcase and OGT, as well as the plasmid-expressing *O*-GlcNAcase from Dr. G. W. Hart. We thank Dr. W. H. Dillmann for sending us an *O*-GlcNAcase adenovirus to compare with ours. We thank John E. DeHaven, Dr. Cynthia Wright, and Dr. Don Menick for their help in developing the *O*-GlcNAcase adenovirus and Dr. Pal Gooz for advice with RNAi. Portions of this work were presented at the 65th Annual Meeting of the American Diabetes Association, June 2005, San Diego, CA (*Diabetes* 54, *Suppl* 1: A324, 2005).

GRANTS

This work was supported by National Institute of Diabetes and Digestive and Kidney Diseases Grant DK-02001 to M. G. Buse. L. E. Ball was supported by a postdoctoral fellowship from the Juvenile Diabetes Research Foundation International.

REFERENCES

1. **Brownlee M.** The pathobiology of diabetic complications: a unifying mechanism. *Diabetes* 54: 1615–1625, 2005.
2. **Buse MG.** Hexosamines, insulin resistance, and the complications of diabetes: current status. *Am J Physiol Endocrinol Metab* 290: E1–E8, 2006.
3. **Comer FI, Hart GW.** Reciprocity between O-GlcNAc and O-phosphate on the carboxyl terminal domain of RNA polymerase II. *Biochemistry* 40: 7845–7852, 2001.
4. **Comer FI, Vosseller K, Wells L, Accavitti MA, Hart GW.** Characterization of a mouse monoclonal antibody specific for O-linked N-acetylglucosamine. *Anal Biochem* 293: 169–177, 2001.
5. **Cooksey RC, Hebert LF, Zhu JH, Wofford P, Garvey WT, McClain DA.** Mechanism of hexosamine-induced insulin resistance in transgenic mice overexpressing glutamine:fructose-6-phosphate amidotransferase: decreased glucose transporter GLUT4 translocation and reversal by treatment with thiazolidinedione. *Endocrinology* 140: 1151–1157, 1999.
6. **Deshayes S, Gerbal-Chaloin S, Morris MC, Aldrian-Herrada G, Charnet P, Divita G, Heitz F.** On the mechanism of non-endosomial peptide-mediated cellular delivery of nucleic acids. *Biochim Biophys Acta* 1667: 141–147, 2004.
7. **Dignam JD, Lebovitz RM, Roeder RG.** Accurate transcription initiation by RNA polymerase II in a soluble extract from isolated mammalian nuclei. *Nucleic Acids Res* 11: 1475–1489, 1983.
8. **Dong DL, Hart GW.** Purification and characterization of an O-GlcNAc selective N-acetyl-beta-D-glucosaminidase from rat spleen cytosol. *J Biol Chem* 269: 19321–19330, 1994.
9. **Gao Y, Wells L, Comer FI, Parker GJ, Hart GW.** Dynamic O-glycosylation of nuclear and cytosolic proteins: cloning and characterization of a neutral, cytosolic beta-N-acetylglucosaminidase from human brain. *J Biol Chem* 276: 9838–9845, 2001.
10. **Garvey WT, Olefsky JM, Matthaei S, Marshall S.** Glucose and insulin co-regulate the glucose transport system in primary cultured adipocytes. A new mechanism of insulin resistance. *J Biol Chem* 262: 189–197, 1987.
11. **Goldberg HJ, Whiteside CI, Hart GW, Fantus IG.** Posttranslational, reversible O-glycosylation is stimulated by high glucose and mediates plasminogen activator inhibitor-1 gene expression and Sp1 transcriptional activity in glomerular mesangial cells. *Endocrinology* 147: 222–231, 2006.
12. **Hazel M, Cooksey RC, Jones D, Parker G, Neidigh JL, Witherbee B, Gulve EA, McClain DA.** Activation of the hexosamine signaling pathway in adipose tissue results in decreased serum adiponectin and skeletal muscle insulin resistance. *Endocrinology* 145: 2118–2128, 2004.
13. **He TC, Kinzler KW, Vogelstein B.** A simplified system for rapid generation of recombinant adenoviruses. A practical guide to using the AdEasy system [Online]. Howard Hughes Medical Institute and Molecular Genetics Laboratory, Johns Hopkins Oncology Center. http://www.coloncancer.org/adeasy/protocol.htm [2006].
14. **He TC, Zhou S, da Costa LT, Yu J, Kinzler KW, Vogelstein B.** A simplified system for generating recombinant adenoviruses. *Proc Natl Acad Sci USA* 95: 2509–2514, 1998.
15. **Hebert LF, Daniels MC, Zhou J, Crook ED, Turner RL, Simmons ST, Neidigh JL, Zhu JS, Baron AD, McClain DA.** Overexpression of glutamine:fructose-6-phosphate amidotransferase in transgenic mice leads to insulin resistance. *J Clin Invest* 98: 930–936, 1996.
16. **Hu Y, Belke D, Suarez J, Swanson E, Clark R, Hoshijima M, Dillmann WH.** Adenovirus-mediated overexpression of O-GlcNAcase improves contractile function in the diabetic heart. *Circ Res* 96: 1006–1013, 2005.
17. **Kreppel LK, Blomberg MA, Hart GW.** Dynamic glycosylation of nuclear and cytosolic proteins. Cloning and characterization of a unique O-GlcNAc transferase with multiple tetratricopeptide repeats. *J Biol Chem* 272: 9308–9315, 1997.
18. **Lubas WA, Frank DW, Krause M, Hanover JA.** O-Linked GlcNAc transferase is a conserved nucleocytoplasmic protein containing tetratricopeptide repeats. *J Biol Chem* 272: 9316–9324, 1997.
19. **Marshall S, Bacote V, Traxinger RR.** Discovery of a metabolic pathway mediating glucose-induced desensitization of the glucose transport system. Role of hexosamine biosynthesis in the induction of insulin resistance. *J Biol Chem* 266: 4706–4712, 1991.
20. **McClain DA.** Hexosamines as mediators of nutrient sensing and regulation in diabetes. *J Diabetes Complications* 16: 72–80, 2002.
21. **McClain DA, Lubas WA, Cooksey RC, Hazel M, Parker GJ, Love DC, Hanover JA.** Altered glycan-dependent signaling induces insulin resistance and hyperleptinemia. *Proc Natl Acad Sci USA* 99: 10695–10699, 2002.
22. **Mitra P, Zheng X, Czech MP.** RNAi-based analysis of CAP, Cbl, and CrkII function in the regulation of GLUT4 by insulin. *J Biol Chem* 279: 37431–37435, 2004.
23. **Nelson BA, Robinson KA, Buse MG.** High glucose and glucosamine induce insulin resistance via different mechanisms in 3T3-L1 adipocytes. *Diabetes* 49: 981–991, 2000.
24. **Nelson BA, Robinson KA, Buse MG.** Insulin acutely regulates Munc18-c subcellular trafficking: altered response in insulin-resistant 3T3-L1 adipocytes. *J Biol Chem* 277: 3809–3812, 2002.
25. **Nelson BA, Robinson KA, Buse MG.** Defective Akt activation is associated with glucose- but not glucosamine-induced insulin resistance. *Am J Physiol Endocrinol Metab* 282: E497–E506, 2002.
26. **Obici S.** Hexosamine pathway contribution to insulin resistance. New insights from muscle specific GFAT transgenic. *65th Annual Meeting of the American Diabetes Association*, San Diego, CA, 2005.
27. **Rossetti L, Giaccari A, DeFronzo RA.** Glucose toxicity. *Diabetes Care* 13: 610–630, 1990.
28. **Rossetti L.** Perspective: Hexosamines and nutrient sensing. *Endocrinology* 141: 1922–1925, 2000.
29. **Toleman C, Paterson AJ, Whisenhunt TR, Kudlow JE.** Characterization of the histone acetyltransferase (HAT) domain of a bifunctional protein with activable O-GlcNAcase and HAT activities. *J Biol Chem* 279: 53665–53673, 2004.
30. **Vosseller K, Wells L, Lane MD, Hart GW.** Elevated nucleocytoplasmic glycosylation by O-GlcNAc results in insulin resistance associated with defects in Akt activation in 3T3-L1 adipocytes. *Proc Natl Acad Sci USA* 99: 5313–5318, 2002.
31. **Wells L, Vosseller K, Hart GW.** Glycosylation of nucleocytoplasmic proteins: signal transduction and O-GlcNAc. *Science* 291: 2376–2378, 2001.
32. **Wells L, Gao Y, Mahoney JA, Vosseller K, Chen C, Rosen A, Hart GW.** Dynamic O-glycosylation of nuclear and cytosolic proteins: further characterization of the nucleocytoplasmic beta-N-acetylglucosaminidase, O-GlcNAcase. *J Biol Chem* 277: 1755–1761, 2002.
33. **Whisenhunt TR, Yang X, Bowe DB, Paterson AJ, Van Tine BA, Kudlow JE.** Disrupting the enzyme complex regulating O-GlcNAcylation blocks signaling and development. *Glycobiology* 16: 551–563, 2006.
34. **Yki-Jarvinen H, Helve E, Koivisto VA.** Hyperglycemia decreases glucose uptake in type I diabetes. *Diabetes* 36: 892–896, 1987.

APPENDIX G

Panomics

Transfection of Differentiated 3T3-L1 Adipocytes using DeliverX Plus siRNA Reagent Solution

Introduction

The usefulness of many interesting phenotypic cell models is limited by the unavailability of an efficient transfection system. One such cell model is the differentiated murine 3T3-L1 adipocyte, which is used for studying insulin signaling, glucose homeostasis and lipid loading. Under appropriate incubation conditions, pre-adipocyte 3T3-L1 cells differentiate into an adipocyte phenotype exhibiting many of the morphological, biochemical, and insulin-responsive features of the normal rodent adipocyte.[1] To date, most siRNA gene silencing experiments in 3T3-L1 cells have been limited to pre-adipocytes because they are relatively easy to transfect using commercially available reagents. Transfection of siRNA into differentiated 3T3-L1 adipocytes, on the other hand, has only been accomplished by electroporation.[1] However, electroporation is expensive, incompatible with high throughput assay formats, and toxic to cells.[2] Here, we report using the DeliverX™ Plus siRNA Transfection Kit in a lower-cost, scalable transfection protocol that successfully delivers siRNA into differentiated 3T3-L1 adipocytes with no apparent effect on cell viability.

The DeliverX Plus siRNA Transfection Kit is based on novel "MPG" delivery technology developed at Centre de Recherches en Biochimie Macromoléculaire (CNRS) in Montpellier (France) in the laboratory of Dr. F. Heitz and Dr. G. Divita. MPG technology uses virus-derived amphipathic peptides that directly interact with nucleic acid cargos to form nanoparticles capable of diffusing through plasma membranes and releasing their contents inside the cell.[1,3–8] The mechanism of entry is receptor-independent, involves MPG/lipid interactions, and avoids the endocytic pathway, thereby preventing endosomal or lysosomal degradation of cargos.[4] The diffusion capability of MPG technology permits efficient and robust siRNA delivery into a wide range of cell types. MPG peptides can be designed to accommodate specific molecular cargos including siRNAs, single and double strand oligonucleotides, plasmids, peptides and proteins.

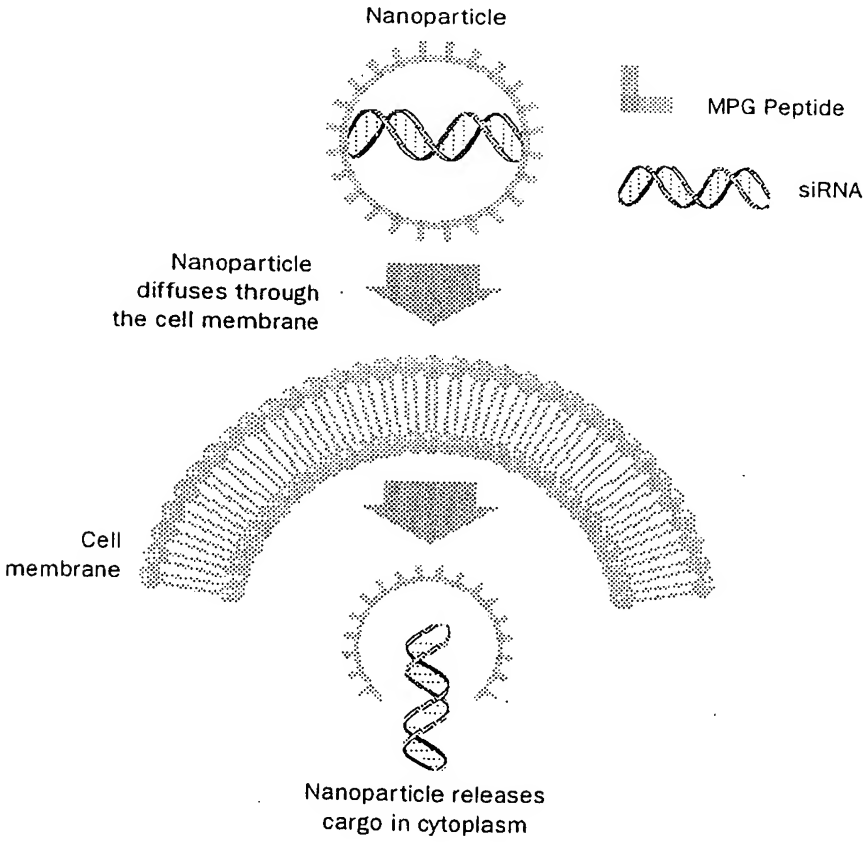

Figure 1. MPG Peptide-Based Delivery Technology

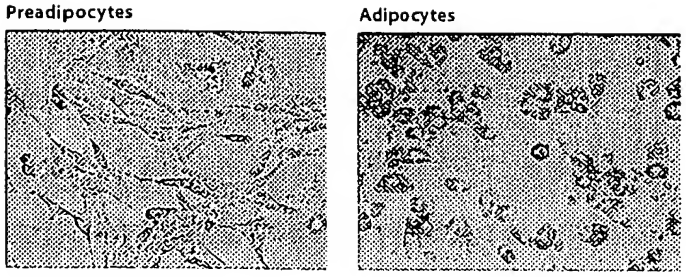

Figure 2. Transformation of 3T3 L1 fibroblasts to adipocytes after induction with isobutylmethine, dexamethasone and insulin (right) fibroblasts with mouse preadipocytes.

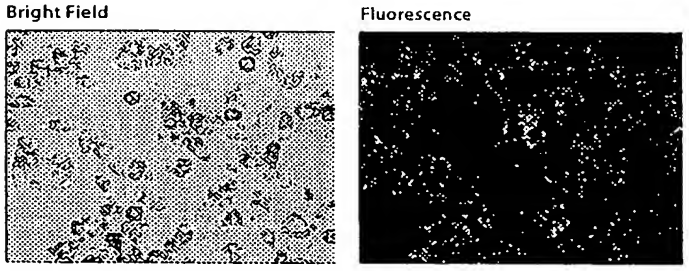

Figure 3. Transfection of FAM-labeled siRNA delivery control into 3T3-L1 adipocytes.

Materials and Methods

GAPDH siRNA was synthesized by Trilink Biotechnologies, Inc. GADPH siRNA negative control and FAM-labeled siRNA Control were obtained from Ambion, Inc. and Panomics, Inc. respectively.

The 3T3-L1 fibroblasts America Type Culture Collection (ATCC) were induced to differentiate according to Jiang et al.[1] Briefly, cells were grown to 100% confluence in an initial culture media, DMEM containing 10% bovine calf serum. At 100% confluence, the initial culture media was replaced with induction media #1, DMEM containing 10% fetal bovine serum (FBS), 5 ug/mL insulin, 0.25 uM dexamethason and 0.5 mM 3-isobutyl-1-methylxanthine. After 2 days incubation at 37°C in 5% CO_2, the induction media #1 was replaced with induction media #2, DMEM containing 10% FBS and 5 ug/uL insulin. After 2 days incubation at 37°C in 5% CO_2, induction media #2 was replace with induction media #1. After 2 days incubation at 37°C in 5% CO_2, induction media #1 was replace with induction media #2. After 8 days of differentiation, greater than 80% of the cells began to build up visible lipid vesicles as shown in Figure 2.

Following trypsinization and treatment with collagenase to reduce clumping, each well of a 96-well microplate was seeded with 5,000-20,000 of the differentiated cells. The microplate was then incubated at 37°C in 5% CO_2 overnight. Transfection was performed according to the DeliverX Plus siRNA Transfection Kit validated protocol. Cells were lysed 24 hours post-transfection and GADPH and cyclophilin B, (PPIB, peptidylpropyl isomerase B), mRNA expression were measured using the QuantiGene® Reagent System according to the manual. We corrected for the differences in the cell number per well by normalizing the GAPDH signal to the PPIB signal.[9] Relative GAPDH expression levels were determined by normalizing measured levels against the siRNA negative control. Transfection and analysis of wells were carried out in triplicate.

Cell viability and proliferation were determined by analyzing PPIB mRNA levels 24 hours after transfection.[9-10] We observed that PPIB levels correlated closely with ATP levels.

Results and Discussion

Differentiated 3T3-L1 adipocytes such as those shown in Figure 2 represent one of the most difficult-to-transfect cell lines[1] used routinely in cell biology studies and were therefore selected to challenge the efficiency of siRNA transfection using the DeliverX Plus Transfection Kit. First, we evaluated the transfection efficiency by determining the percentage of cells containing the FAM-labeled siRNA delivery control as determined by fluorescence and bright field imaging. The results shown in Figure 3 indicate transfection of FAM-labeled siRNA Control into more than 90% of the differentiated adipocytes.

Next, we assessed functional transfection efficiency using siRNA-mediated gene silencing. While typical functional assays for siRNA transfection efficiency often use reporter genes such as luciferase or GFP, the transfection of reporter genes is not always uniform across all the cells in a microplate well, and the expression level can be low and transient. Therefore we selected GAPDH gene silencing in differentiated 3T3-L1 adipocytes as a model system for measurement of functional transfection efficiency. GAPDH mRNA is highly and constitutively expressed and therefore presents a more reliable and diagnostic knockdown challenge.

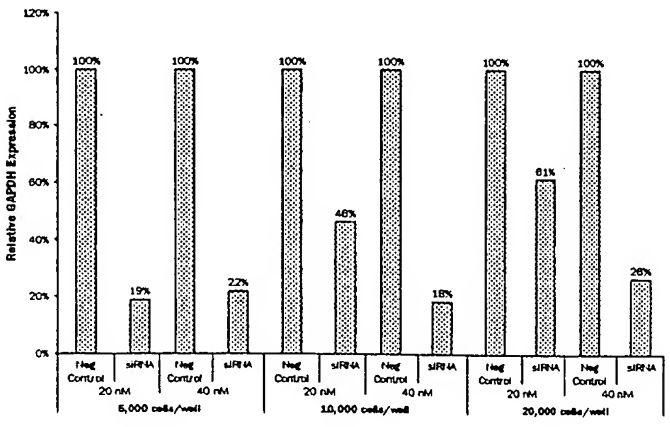

Figure 4. Silencing GAPDH gene expression using DeliverX Plus siRNA Transfection Kit.

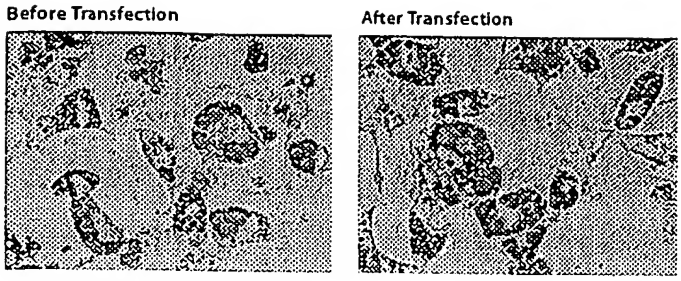

Figure 5. Analysis of cell morphology 24 hours after transfection.

We transfected 20–40 nM GAPDH siRNA into microplate wells containing 5,000–20,000 adipocytes. We verified that at least 85% of cells per well exhibited the adipocyte phenotype, lipid vesicles, during the transfection. Twenty-four hours after transfection, we observed significant GAPDH gene knockdown at all cell densities. The data shown in Figure 4 indicate that DeliverX Plus siRNA Transfection Kit robustly delivered siRNA into differentiated adipocytes, producing a knockdown effect of greater than 80% in wells containing 5,000 to 10,000 cells.

Finally, we evaluated the effect of the DeliverX Plus siRNA Transfection Reagent on cell viability and morphology. Figure 5 shows that 3T3-L1 cell morphology did not change following transfection using DeliverX Plus siRNA Transfection Kit. In addition, cell viability and proliferation remained comparable between transfected and non-transfected cells, as shown in Figure 6.

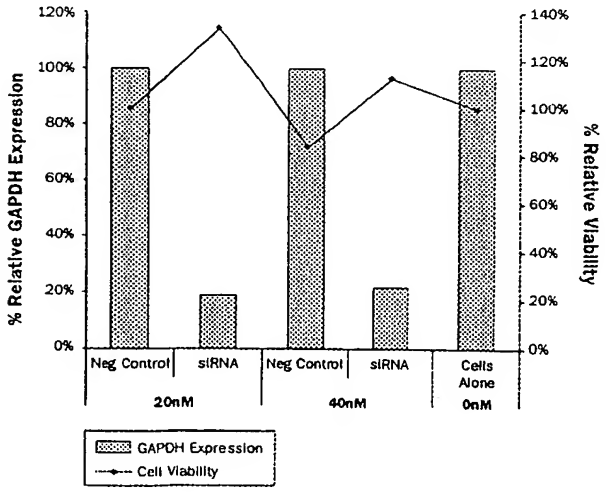

Figure 6. Cell viability and silencing of GAPDH gene 24 hours after transfection.

Table 1: Cell types transfected with DeliverX Plus siRNA Transfection Kit using validated cell-type specific protocols.

3T3-L1	differentiated mouse adipocytes
C2C12	differentiated mouse myotubes
C2C12	undifferentiated mouse myocytes
RAW 264.7	mouse macrophage cells
U87MG	human brain glioblastoma astrocytoma cells
NHEK-AD	primary human adult keratinocytes
THP-1	human peripheral blood acute monocytic leukemia cells
HUVEC	human umbilical vein endothelial cells
MDA-MB-231	human breast adenocarcinoma cells
MCF-7	human breast carcinoma cells
HT29	human colon carcinoma cells
SW620	human colon carcinoma cells
HepG2	human hepatocarcinoma cells
BSMC	human bronchial smooth muscle cells
A549	human lung carcinoma cells
A2780	human ovarian cancer cells
ASPC-1	human pancreatic carcinoma cells

All validated cell-specific protocols meet the specification of ≥ 70% mRNA knockdown of GAPDH 24 hours post transfection and ≥70% cell viability.

Summary

We have demonstrated that DeliverX Plus siRNA Transfection Kit delivers siRNA into difficult-to-transfect, differentiated adipocytes. We observed greater than 90% transfection efficiency and more than 80% siRNA-mediated gene silencing over a wide range of cell densities with no apparent impact on cell morphology and viability. As shown in Table 1, similar results have been obtained with other difficult-to-transfect cell lines. In conclusion, DeliverX Plus siRNA Transfection Kit was demonstrated to be an effective, robust, and gentle transfection reagent for classically difficult-to-transfect cell types.

Panomics

6519 Dumbarton Circle

Fremont, CA 94555

Toll Free: 1.877 PANOMICS (1.877.726.6642)

T: 510.818.2600

F: 510.818.2610

References

1. Jiang, Z.Y., Zhou, Q.L., Coleman, K.A., Chouinard, M., Boese, Q., Szech, M.P., (2003), Insulin signaling through Akt/protein kinase B analyzed by small interfering RNA-mediated gene silencing, PNAS, Vol 100, 7569-7574.

2. www.bio.davidson.edu/courses/molbiol/MolStudents/spring2003/Mccord/electroporation.html

3. Morris, M.C., Vidal, P., Chaloin, L., Heitz, F., Divita, G., (1997), A new peptide vector for efficient delivery of oligonucleotides into mammalian cells, Nucl. Acids Res, Vol 25, 2730-2736.

4. Morris, M.C., Chaloin, Mery, J., Heitz, F., Divita, G., (1999), A novel potent strategy for gene delivery using a single peptide vector as a carrier, Nucl. Acids Res, Vol 27, 3510-3517.

5. Simeoni, F., Morris, M.C., Heitz, F., Divita, G., A insight into the mechanism of the peptide-based gene delivery system MPG: implications for delivery of siRNA into mammalian cells, Nucl. Acids Res, Vol 31, 2717-2724, (2003).

6. Morris, K.V., Chan, S.W., Jacobsen, S.E., Looney, D. J., (2004), Small interfering RNA-induced transcriptional gene silencing in human cells, Science, Vol 305, 1289-1291.

7. Morris, M.C., Robert-Hebmann, V., Chaloin, L., Mery, J., Heitz, F., Devaux, C., Goody, R.S., Divita, G., (1999), A new potent HIV-1 reverse transcriptase inhibitor, J Biol Chem, Vol 274, 24941-24946.

8. Deshayes S, Gerbal-Chaloin S, Morris MC, Aldrian-Herrada G, Charnet P, Divita G, Heitz F., On Mechanism of non-endosomial peptide-mediated cellular delivery of nucleic acids. Biochem Biophys Acta. 1667, 141-7.

9. Pachot A., Blond J.L., Mougin B., Miossec P., (2004), Peptidylpropyl Isomerase B (PPIB),: suitable reference gene for mRNA quantification in peripheral whole blood. J. Biotechnol., Vol 114, 121-4.

10. Horibe, T., Yosho, C., Okada, S., Tsukamoto, M., Nagai, H., Hagiwara, Y., Tojimoto, Y., Kikuchi, M., (2002), The Chaperone Activity of Protein Disulfide Isomerase is Affected by Cyclophilin B and Cyclophilin A in Vitro, J. Chem. Vol 132, 401-407.

AUTHORS:
Larry Pastor, Rajesh Chavli, Gilles Divita, Wehai He, Frederic Heitz, Gary McMaster, May Morris, Quan Nguyen, Federica Simeoni, and Alguo Zhang.

Ordering Information

Product	Size	Catalog No.
DeliverX Plus siRNA Transfection Evaluation Kit	0.12 mL*	DX0051
DeliverX Plus siRNA Transfection Kit	0.4 mL	DX0052
DeliverX Plus siRNA Transfection Kit	1.0 mL	DX0053
DeliverX Plus siRNA Transfection Kit	4 x 1.0 mL	DX0054
FAM-labeled siRNA Control	0.12 mL	DX0100
Sonicator X100	each	DX0400

*0.12 mL DeliverX Plus siRNA Transfection Reagent and validated cell-type specific protocols, 0.12 mL FAM-labeled siRNA Control, 0.06 mL Human GADPH siRNA Control